8-1-1998

Hot White Dwarfs in the Extreme - Ultraviolet Explorer Survey. IV. DA White Dwarfs with Bright Companions

Stephane Vennes
University of California - Berkeley

Damian J. Christian
University of California - Berkeley

John R. Thorstensen
Dartmouth College

THE ASTROPHYSICAL JOURNAL, 502:763–787, 1998 August 1

HOT WHITE DWARFS IN THE *EXTREME-ULTRAVIOLET EXPLORER* SURVEY. IV. DA WHITE DWARFS WITH BRIGHT COMPANIONS

STÉPHANE VENNES
Space Sciences Laboratory, University of California, Berkeley, CA 94720-7450, and Astrophysical Theory Centre, Australian National University, Canberra, ACT 0200, Australia; vennes@ssl.berkeley.edu

DAMIAN J. CHRISTIAN
Center for EUV Astrophysics, 2150 Kittredge Street, University of California, Berkeley, CA 94720-5030; damian@cea.berkeley.edu

AND

JOHN R. THORSTENSEN
Department of Physics and Astronomy, Dartmouth College, Hanover, NH 03755; thorsten@dartmouth.edu
Received 1997 August 18; accepted 1998 March 9

ABSTRACT

We present an analysis of optical, ultraviolet, and X-ray spectral properties of a sample of 13 hot hydrogen-rich (DA) white dwarfs, each paired with a luminous unresolved companion. Using low-dispersion *International Ultraviolet Explorer* spectra, *ROSAT* photometry, and *Extreme-Ultraviolet Explorer* photometry and spectroscopy, we estimate the effective temperature, mass, and distance of the white dwarfs. Additionally, we examine the question of their atmospheric composition. We establish orbital properties for most binaries by means of high-dispersion optical spectroscopy obtained with the Hamilton echelle spectrograph at Lick Observatory; the same data help uncover evidence of activity in some of the secondary stars that is also notable in *ROSAT* X-ray measurements. In particular, we find high-amplitude (>20 km s^{-1}) velocity variations in only two stars (HD 33959C and HR 8210), low-amplitude variations in four additional objects (HD 18131, HR 1608, θ Hya, and BD $+27°1888$), and no variations (<2 km s^{-1}) in the remainder. We have observed Ca H and K in emission in four (BD $+08°102$, HD 18131, HR 1608, and EUVE J0702+129) of the six objects that were also detected in the 0.52–2.01 keV *ROSAT* PSPC band, while the source of the hard X-ray emission in HD 33959C remains unknown; other investigators have noted some evidence of activity in the remaining 0.52–2.01 keV detection, HD 217411. Properties of the white dwarfs are also investigated; EUV spectroscopy shows the effect of a low heavy element abundance in the atmosphere of the white dwarf in HD 33959C and of a high heavy element abundance in HD 223816; measurements of all other objects are apparently consistent with emission from pure-hydrogen atmospheres. However, current data do not constrain well the white dwarf parameters, and, to remedy the situation, we propose to obtain spectroscopy of the complete H Lyman line series.

Subject headings: binaries: general — stars: evolution — stars: fundamental parameters — ultraviolet: stars — white dwarfs — X-rays: stars

1. INTRODUCTION

Recently, the *ROSAT* WFC and *Extreme-Ultraviolet Explorer* (*EUVE*) sky surveys have produced samples of white dwarfs selected by their extreme-ultraviolet (EUV) emission (Pye et al. 1995; Bowyer et al. 1996; Lampton et al. 1997). These samples show many distinctive and interesting properties—white dwarfs of the upper end of the luminosity function, membership in multiple systems, most often composed of main-sequence stars and exotic chemical composition and stellar masses. Most notably, a number of white dwarfs paired with normal- and high-mass (K IV, G IV–V, F IV–V, A III–V), or low-mass (M V, K V) secondary stars have been identified. Many of these objects bear orbital characteristics of post–common-envelope (CE) binaries. Vennes & Thorstensen (1994a, 1995) studied the sample properties of five close DA + dMe/dKe binaries selected at EUV wavelengths. The systems emerged from a post-CE phase with orbits of the order of 1 day and normal stellar masses. The observed mass and period distributions may constrain the theory of binary evolution (see de Kool & Ritter 1993) and set the initial conditions for the formation of cataclysmic variables (see King et al. 1994). Other binaries with massive secondary stars are not as well studied, despite their brightness at optical wavelengths. These systems, composed of a DA white dwarf and a secondary star with spectral types from B to K and luminosity classes from V to III, have all been identified in low-resolution *International Ultraviolet Explorer* (*IUE*) far-ultraviolet (FUV) spectroscopy. Fleming et al. (1991) first reported a white dwarf companion (RE J1111−224) to the bright A star β Crateris and drew a parallel with the famous Sirius A1 V + DA pair. Webbink et al. (1992); Hodgkin et al. (1993); Wonnacott, Kellett, & Stickland (1993); and Landsman, Simon, & Bergeron (1993) identified white dwarf companions to the F stars HD 33959C and HD 15638, the A star HR 8210, and the K0 IV star HR 1608. The known single-line binary HR 8210 (Harper 1927) therefore revealed itself to be hiding a massive DA white dwarf ($M \geq 1.1\ M_{\odot}$). Other systems were soon identified (Barstow et al. 1994; Vennes et al. 1995, 1997a; Génova et al. 1995; Christian et al. 1996), and a growing sample, now over a dozen objects, is available. A systematic study of the stellar and binary properties will allow us to draw useful parallels with the EUV-selected sample of isolated white dwarfs (Vennes et al. 1996a, 1997b).

We present the results of an extensive multiwavelength

TABLE 1

SAMPLE OF BINARIES

Name[a]	HD Name	Other Name	V	Spectral Type	References
EUVE J0044+095.....	...	BD +08°102	10.16	K2 V	1, 2
EUVE J0228−613.....	HD 15638	CD −61°431	8.8	F6 V	3
EUVE J0254−053.....	HD 18131	BD −05°541	7.2	K0 III–IV	4
EUVE J0459−102.....	HD 32008	HR 1608	5.38	K0 IV	3
EUVE J0515+326.....	HD 33959C	14 Aur C	7.95	F4 IV–V	5, 6
EUVE J0702+129.....	...	2RE	10.0	K0 IV–V	7
EUVE J0914+023.....	HD 79469	θ Hya	3.88	B9.5 V	8 (2RE)
EUVE J1024+263.....	HD 90052	BD +27°1888	9.6	F0 V	9
EUVE J1111−228.....	HD 97277	β Crt	4.48	A1 III	10
EUVE J1925−565.....	...	2RE	10.6	G5 (V)	1
EUVE J2126+193.....	HD 204188	HR 8210	6.07	A8 V	11, 3
EUVE J2300−070.....	HD 217411	BD −07°5906	9.8	G5 (V)	1
EUVE J2353−703.....	HD 223816	CD −71°1808	8.8	G0 V	1

[a] Bowyer et al. 1996.

REFERENCES.—(1) Barstow et al. 1994; (2) Kellett et al. 1995; (3) Landsman et al. 1993; (4) Vennes et al. 1995; (5) Webbink et al. 1992; (6) Hodgkin et al. 1993; (7) Vennes et al. 1997a; (8) Pye et al. 1995; (9) Burleigh et al. 1997; (10) Fleming et al. 1991; (11) Wonnacott et al. 1993.

observation campaign of a sample of 13 binaries comprising a hot DA white dwarf and a luminous secondary star. We present new low- and high-dispersion optical spectroscopy supporting spectral type and activity classification, and a study of the orbital properties (§ 2.1 and § 2.2). In § 2.3 and § 2.4 we present new and archival EUV and FUV observations, as well as recently released *ROSAT* all-sky survey observations. In § 3, we analyze the complete spectral energy distribution. We examine the likely stellar parameters for the white dwarfs and luminous secondary stars; we also search for evidence of activity in the secondary stars. In § 4 we determine the binary properties. Finally, we conclude in § 5 and propose additional optical, FUV, and EUV observations.

2. OBSERVATIONS

Table 1 lists a sample of 13 hot DA white dwarf plus luminous secondary binaries selected from the *EUVE* all-sky survey. We obtained high- and low-dispersion optical spectra with a resolution of $\Delta\lambda \sim 0.1$ and 5 Å. We also searched the *IUE* final archives at NASA/GSFC and ESA/VILSPA for low-dispersion FUV spectra ($\Delta\lambda \sim 6$ Å); finally, we obtained medium-dispersion EUV spectra ($\lambda/\Delta\lambda \sim 200$–300) from the *EUVE* spectroscopic archives. We also obtained new EUV spectra of the DA + G binary EUVE J1925−565 during the fouth *EUVE* guest observer cycle and FUV spectra of EUVE J0702+129 during the *IUE* 19th episode. The data are described below. As a convention, we will refer to the pre-EUV catalog designation for the bright secondary stars and to the *EUVE* catalog designation for the white dwarf primary stars.

Table 2 lists other binaries of interest selected from the *EUVE* all-sky survey. Some of these objects share a number of properties with our main sample (Table 1) and will eventually be subjected to similar studies. Note that 2RE 0357+283 (EUVE J0357+286) includes a fast rotating G2 V star (Jeffries & Stevens 1996; Jeffries & Smalley 1996). Note also the sample of short-period binaries ($P \sim 1$ day): Feige 24, V471 Tau, EUVE J0720−317, EUVE J1016−053, and EUVE J2013+400. Schultz, Zuckerman, & Becklin (1996) determined that the binaries GD 984, GD

TABLE 2

OTHER BINARIES IN THE *EUVE* SURVEY

Binary	Other Name	Secondary Type	V	References
EUVE J0134−161	GD 984	dMe	13.8	1
EUVE J0235+037[a].....	Feige 24	dMe	12.42	2
EUVE J0350+172[a].....	V 471 Tau	K2 V	9.2	3
EUVE J0356−366	MS 0354.6−3650	G2 V	12.45	4
EUVE J0357+286	2RE 0357+283	K2 V	11.7	5
EUVE J0645−167	α CMa	A1 V	−1.47	6
EUVE J0720−317[a].....	2RE 0720−314	dMe	14.8	7
EUVE J0729−388	y Pup	B5 V	5.42	8
EUVE J0827+284	PG 0824+289	dC	14.73	9
EUVE J1016−053[a].....	2RE 1016−052	dMe	14.2	10
EUVE J1027+323	2RE 1027+322	G5 V	13.0	11
EUVE J1036+461	GD 123	dK	13.15	1
EUVE J1629+780	2RE 1629+780	dMe	13.0	12
EUVE J2013+400[a].....	2RE 2013+400	dMe	14.2	13

[a] Short-period binaries.

REFERENCES.—(1) Schultz et al. 1996; (2) Vennes & Thorstensen 1994b; (3) Nelson & Young 1970; (4) Christian et al. 1996; (5) Jeffries, Burleigh, & Robb 1996; (6) Thejll & Shipman 1986; (7) Vennes & Thorstensen 1994a, 1996; (8) Vennes, Berghöfer, & Christian 1997; (9) Heber et al. 1993; (10) Tweedy et al. 1993; Thorstensen, Vennes, & Bowyer 1996; (11) Génova et al. 1995; (12) Sion et al. 1995; (13) Thorstensen, Vennes, & Shambrook 1994.

123, and 2RE 1629+780, lacking radial velocity variations, are probably not in close orbits.

2.1. *Low-Dispersion Optical Spectroscopy (MDM, Lick, MSO)*

We observed the EUV-selected sample of binaries at the Michigan-Dartmouth-MIT (MDM) Observatory from 1996 January 6 to 12 (UT) with the Hiltner 2.4 m telescope. We used the Mark III spectrograph and a Tek 1024 × 1024 CCD with a wavelength coverage between 3600 and 6000 Å at 2.32 Å pixel^{-1}, or a spectral resolution of 5–6 Å. We used the sum of Hg-Ne and Xe lamps to extract the wavelength scale.

On 1996 December 18 and 19 (UT) we observed with the Lick Observatory 3 m telescope. We used the double spectrograph with a 1200 × 400 Reticon CCD and a 452 lines mm^{-1} grism on the blue side covering the wavelength range 3350–6470 Å at 2.54 Å pixel^{-1}, or 5 Å resolution.

We then observed with the 74 inch (1.9 m) telescope at Mount Stromlo Observatory (MSO) on 1997 April 1–3 (UT), and October 1–6 (UT). We used the spectrograph mounted at the Cassegrain focus with a 300 lines mm^{-1} grating and a UVAR 1752 × 532 thinned SITe CCD binned 2 × 2 (2.72 Å pixel^{-1}). Fe-Ar comparison lamps were obtained after each exposure; the spectra cover the range 3710–6110 Å at 5–6 Å resolution; the October spectra were truncated at 3800–5160 Å.

All images were bias-subtracted, flat-fielded, and all spectra were extracted and wavelength- and flux-calibrated using NOAO's IRAF at the Center for EUV Astrophysics (Berkeley) and at the Astrophysical Theory Centre (Canberra).

2.2. *High-Dispersion Optical Spectroscopy (Lick, MSO)*

Between 1995 October and 1997 December, we observed 10 objects from the sample of binaries using the 24 inch coudé auxiliary telescope (CAT) and the Hamilton echelle spectrograph (Vogt 1987). We used a 2048 × 2048 CCD binned 2 × 2 with a dispersion of 0.033 Å pixel^{-1} at Ca H and K and 0.054 Å pixel^{-1} at Hα; the resulting velocity resolution is 7.5 km s^{-1}. The spectra were wavelength-calibrated with Th-Ar spectra and flat-fielded with quartz spectra. We obtained IAU velocity standards and established the accuracy of the velocity scale.

A similar program was initiated at the MSO 74 inch telescope in 1997 November. We used the 32 inch camera at the coudé focus and a 600 lines mm^{-1} grating, resulting in a dispersion of 0.152 Å pixel^{-1} at Hα in the second order and 0.102 Å pixel^{-1} at Ca H and K in the third order. The spectra were wavelength calibrated with Cu-Ar spectra and flat-fielded with quartz spectra. The resulting velocity resolution is 13.8 km s^{-1} at Hα and 15.6 km s^{-1} at Ca H and K. We obtained a few initial radial velocity measurements of HD 15638, HD 223816, and EUVE J1925−565 in 1997 November and December.

2.3. *FUV Spectroscopy (IUE)*

Low-dispersion FUV spectra were obtained from the *IUE* final archives at NASA/GSFC and ESA/VILSPA. We also obtained high-dispersion spectra of HR 1608 and β Crt from the original archives. The spectra from the final archives were processed with standard "NEWSIPS" (Nichols & Linsky 1996). The high-dispersion spectra processed with the original "IUESIPS" were binned to 3 Å to match the low dispersion.

Table 3 summarizes FUV and optical observations obtained for our sample of binaries.

2.4. *EUV/Soft X-Ray Photometry (EUVE, ROSAT) and EUV Spectroscopy (EUVE)*

Table 4 compiles EUV photometric data from the Bowyer et al. (1996) and Pye et al. (1995) catalogs of EUV sources: the *EUVE* Lexan and Al/C bands centered on 100 and 200 Å, respectively, and the *ROSAT* WFC S1 and S2 bands centered on 90 and 160 Å, respectively. Table 4 also presents *ROSAT* PSPC count rates in two separate bands derived from Voges et al. (1997)—the soft X-ray (0.1–0.4 keV) and hard X-ray (0.5–2.0 keV) bands.

EUVE spectra were obtained from the public archive at the Center for EUV Astrophysics in Berkeley. The short-wavelength (SW) spectrometer covers 70–190 Å with a resolution of 0.47 Å. The medium-wavelength (MW) spectrometer covers 140–380 Å with a resolution of 0.94 Å. The long-wavelength (LW) spectrometer covers 280–760 Å with a resolution of ∼2 Å. The *EUVE* spectra were reduced from the standard data products in *ST* (i.e., *Space*

TABLE 3

OPTICAL AND FUV OBSERVATIONS

Name	Optical (Å)	Echelle	*IUE* SWP	*IUE* LWP
EUVE J0044+095.....	3350–6470	Hα, Ca H and K	45396	23739
EUVE J0228−613.....	3710–6110	Hα, Ca H and K	45007	24027
EUVE J0254−053.....	3600–6000	Hα, Ca H and K	52158	29200
EUVE J0459−102.....	3710–6110	Hα, Ca H and K	46680	...
				LWR11254H[a]
EUVE J0515+326.....	3600–6000	Hα, Ca H and K	45690	23959
EUVE J0702+129.....	3600–6000	Hα, Ca H and K	56186	31689
EUVE J0914+023.....	3600–6000	Hα, Ca H and K	...	...
EUVE J1024+263.....	3350–6470	Hα, Ca H and K	56261	31785
EUVE J1111−228.....	3600–6000	Hα, Ca H and K	45147	...
			51276H[a]	28518H[a]
EUVE J1925−565.....	3710–6110	Hα	49048	...
EUVE J2126+193.....	3350–6470	Hα, Ca H and K	50899	28268
EUVE J2300−070.....	3800–5160	Hα, Ca H and K	46146	...
EUVE J2353−703.....	3800–5160	Hα, Ca H and K	45962	24107

[a] High-dispersion spectra degraded to low dispersion.

TABLE 4

EUV/X-RAY PHOTOMETRIC OBSERVATIONS

	EUVE[a]		*ROSAT* WFC[b]		*ROSAT* PSPC[c]	
NAME	100 Å (counts s^{-1})	200 Å (counts s^{-1})	S1 (counts s^{-1})	S2 (counts s^{-1})	0.11–0.41 keV (counts s^{-1})	0.52–2.01 keV (counts s^{-1})
EUVE J0044+095.....	0.038 ± 0.011	0.033 ± 0.014:	0.016 ± 0.005	0.013 ± 0.005	0.199 ± 0.071	0.207 ± 0.035
EUVE J0228−613.....	1.182 ± 0.029	0.093 ± 0.012	0.675 ± 0.035	1.104 ± 0.036	5.217 ± 0.257	≤0.027
EUVE J0254−053.....	0.137 ± 0.014	0.044 ± 0.012:	0.065 ± 0.013	0.127 ± 0.021	0.238 ± 0.062	0.058 ± 0.021
EUVE J0459−102.....	0.149 ± 0.020	0.051 ± 0.016:	0.065 ± 0.007	0.216 ± 0.014	0.358 ± 0.067	0.173 ± 0.028
EUVE J0515+326.....	0.393 ± 0.023	0.135 ± 0.017	0.884 ± 0.023	2.753 ± 0.042	4.950 ± 0.134	0.101 ± 0.027
EUVE J0702+129.....	0.124 ± 0.015	0.028 ± 0.013:	0.074 ± 0.007	0.112 ± 0.011	0.665 ± 0.069	0.104 ± 0.022
EUVE J0914+023.....	0.122 ± 0.015	0.042 ± 0.014:	0.052 ± 0.007	0.148 ± 0.012	0.124 ± 0.028	≤0.004
EUVE J1024+263.....	0.046 ± 0.010	...	0.033 ± 0.005	0.019 ± 0.007	0.150 ± 0.024	≤0.002
EUVE J1111−228.....	0.316 ± 0.021	0.065 ± 0.017	0.151 ± 0.013	0.459 ± 0.022	0.469 ± 0.050	≤0.007
EUVE J1925−565.....	0.890 ± 0.026	...	0.710 ± 0.038	0.697 ± 0.040	6.790 ± 0.651	≤0.074
EUVE J2126+193.....	0.626 ± 0.028	0.392 ± 0.030	0.263 ± 0.016	0.757 ± 0.025	1.052 ± 0.068	≤0.005
EUVE J2300−070.....	0.069 ± 0.014	0.032 ± 0.016:	0.042 ± 0.009	0.043 ± 0.009	0.311 ± 0.057	0.064 ± 0.020
EUVE J2353−703.....	0.428 ± 0.021	0.929 ± 0.032	0.308 ± 0.022	0.667 ± 0.030	0.056 ± 0.020	≤0.007

[a] Bowyer et al. 1996.
[b] Pye et al. 1995.
[c] Voges et al. 1997.

Telescope) tables format. These tables include a list of tagged photon arrival times, and spacecraft aspect and telemetry information. The tables were processed with the current reduction software (version 1.13). The tables were then converted to quick position event (QPOE) files, which are time-tagged list of photon events in detector coordinates, using the EUV reduction software package (version 1.6.2). Finally, the images were remapped onto celestial coordinates using the spacecraft aspect solution. We then extracted a two-dimensional spectrum using a narrow source aperture and subtracting the background averaged over a region located above and below the source aperture. The spectra were converted from counts versus pixels to flux units versus wavelengths using the current effective area and wavelength solution for each spectrometer. The *EUVE* observation log is given in Table 5.

3. ENERGY DISTRIBUTION (60–6000 Å)

Figures 1*a*–1*m* show the combined optical and ultraviolet energy distributions of 12 composite binary spectra and a spectrum of the high–proper-motion blue star θ Hya. In general, the far- and extreme-ultraviolet ranges are dominated by the hydrogen-rich DA white dwarf; a representative white dwarf model atmosphere illustrates the relative importance of the white dwarf at these wavelengths. The combination of white dwarf flux at ≤1300 Å and the EUV energy distribution constrains the white dwarf parameters. By comparing our optical spectra to the library of optical spectra of Jacoby, Hunter, & Christian (1984), we determine approximate secondary spectral types and luminosity classes (Fig. 1).

The photometric distances are critically compared to recent *Hipparcos* (ESA 1997) parallax measurements. Table 6 lists parallaxes, inferred distances, and proper motions of stars included in the *Hipparcos* catalog. Proper assessment of the data would require that we take into account the yet *unknown* orbital elements of the binaries in our sample, which may introduce systematic errors in parallax or proper-motion measurements. For example, a binary comprising a 1.5 $M_\odot$ secondary and 0.6 $M_\odot$ white dwarf with a 1 yr period has an orbital separation of ∼1.3 AU. At a distance of 100 pc, the separation corresponds to an apparent secondary motion of 4 mas, comparable to the actual parallax (10 mas). A large discrepancy between parallax measurements or between a parallax and a photometric distance may be indicative of orbital motion; availability of several independent parallax or proper-motion measurements helps determine the extent of the problem for a given system.

3.1. *Secondary Star Parameters and Activity*

BD +08°102.—(Fig. 1*a*) The primary star of this binary is the prototype of a new class of fast-rotating stars paired with an evolved companion in a wide binary (Jeffries & Stevens 1996). Kellett et al. (1995) measured a rotational velocity $v_{\rm rot}$ sin $i = 90 \pm 10$ km s^{-1} and no radial velocity variations. We measured a rotational velocity of $v_{\rm rot}$ sin

TABLE 5

EUV SPECTROSCOPIC OBSERVATIONS

Binary	Exposure (10^3 s)	Beginning (UT)	End (UT)
EUVE J0228−613.....	89	1993 Sep 02 14:58	1993 Sep 05 13:32
EUVE J0515+326.....	49	1993 Jan 24 12:00	1993 Jan 26 11:54
EUVE J1925−565.....	53	1996 Jun 15 20:14	1996 Jun 17 22:34
	27	1996 Jun 17 23:58	1996 Jun 19 01:18
	40	1996 Jun 25 07:26	1996 Jun 26 20:58
EUVE J2126+193.....	85	1993 Jul 23 23:16	1993 Jul 27 10:02
EUVE J2353−703.....	61	1993 Aug 06 12:00	1993 Aug 08 8:44

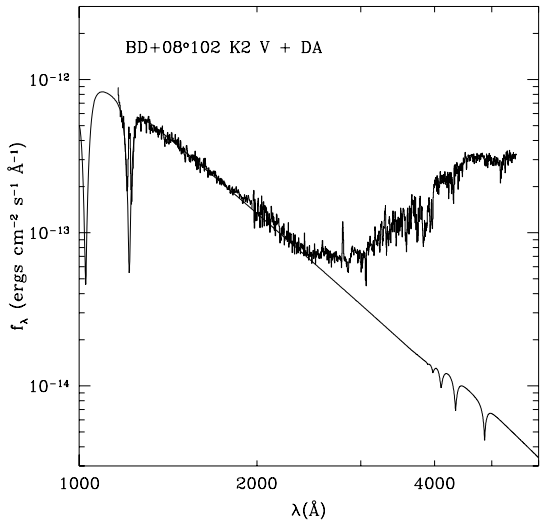

FIG. 1*a*

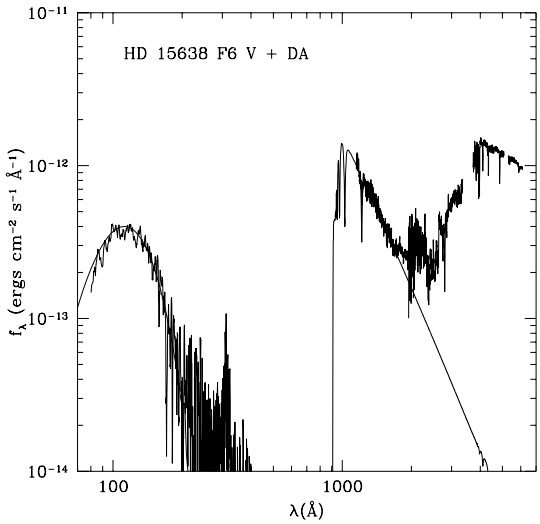

FIG. 1*b*

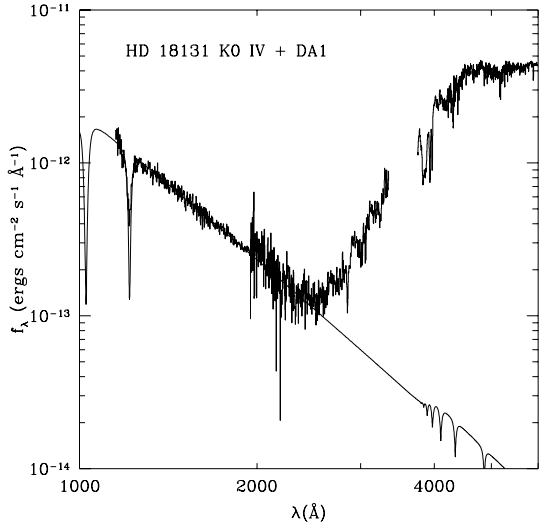

FIG. 1*c*

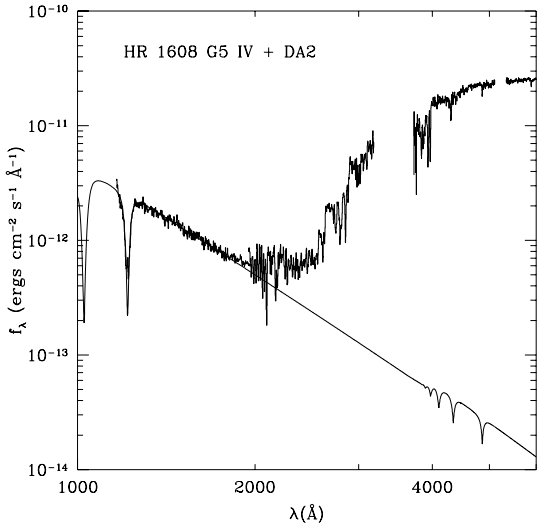

FIG. 1*d*

FIG. 1.—(*a*) Energy distribution of the binary BD +08°102 showing the relative contribution of the white dwarf and luminous companion star: optical spectroscopy ($\lambda > 3500$ Å; $\Delta\lambda \sim 5$ Å), FUV spectroscopy ($1150 < \lambda < 3350$ Å; $\Delta\lambda \sim 6$ Å). A representative pure-H white dwarf model at $T_{\rm eff} = 30{,}000$ K and $\log g = 9.0$ is also shown. Note Mg II emission in the *IUE* spectrum. (*b*) As (*a*), but for HD 15638 and a model at $T_{\rm eff} = 47{,}000$ K and $\log g = 8.0$. EUV spectroscopy ($70 < \lambda < 400$ Å; $\Delta\lambda/\lambda \sim 200$) reveals continuum emission from the hot white dwarf. (*c*) As (*a*), but for HD 18131 and a model at $T_{\rm eff} = 30{,}000$ K and $\log g = 7.5$. (*d*) As (*a*), but for HR 1608 and a model at $T_{\rm eff} = 30{,}000$ K and $\log g = 8.5$. (*e*) As (*a*), but for HD 33959C and a model at $T_{\rm eff} = 44{,}000$ K and $\log g = 8.0$. Note evidence of trace elements ($\lambda < 190$ Å) in the EUV spectrum of the white dwarf. (*f*) As (*a*), but for EUVE J0702+129 and a model at $T_{\rm eff} = 32{,}000$ K and $\log g = 8.0$. (*g*) As (*a*), but for θ Hya and a model at $T_{\rm eff} = 30{,}000$ K and $\log g = 9.0$ and normalized at $V = 15.25$. (*h*) As (*a*), but for BD +27°1888 and a model at $T_{\rm eff} = 36{,}000$ K and $\log g = 8.0$. (*i*) As (*a*), but for β Crt and a model at $T_{\rm eff} = 36{,}000$ K and $\log g = 7.5$. *Voyager* data (900–1100 Å) from Barstow et al. (1994) are added as an illustration. (*j*) As (*a*), but for EUVE J1925−565 and a model at $T_{\rm eff} = 52{,}000$ K and $\log g = 8.0$. (*k*) As (*a*), but for HR 8210 and a model at $T_{\rm eff} = 35{,}000$ K and $\log g = 9.0$. (*l*) As (*a*), but for HD 217411 and a model at $T_{\rm eff} = 40{,}000$ K and $\log g = 8.5$. (*m*) As (*a*), but for HD 223816 and a pure-H model at $T_{\rm eff} = 68{,}000$ K and $\log g = 8.0$. Note evidence of trace elements ($\lambda < 270$ Å) in the EUV spectrum of the white dwarf.

TABLE 6

Hipparcos PARALLAX AND PROPER-MOTION MEASUREMENTS

Name	π (mas)	d (pc)	μ_α (mas)	μ_δ (mas)
HD 15638.....	5.02 ± 0.70	199^{+32}_{-24}	-7.66 ± 0.69	$+9.29 \pm 0.76$
HD 18131.....	9.57 ± 1.26	104^{+16}_{-12}	$+34.68 \pm 1.10$	-21.92 ± 1.20
HR 1608	18.29 ± 1.09	55 ± 3	$+19.49 \pm 0.96$	-136.75 ± 0.77
HD 33959A.....	12.14 ± 1.17	82^{+9}_{-7}	-27.05 ± 1.27	$+12.47 \pm 0.75$
HD 33959C.....	39.77 ± 22.40	25^{+32}_{-9}	-12.50 ± 23.72	$+13.16 \pm 12.19$
θ Hya	25.34 ± 0.97	40 ± 2	$+112.57 \pm 1.41$	-306.07 ± 1.20
β Crt	12.26 ± 0.75	82 ± 5	$+4.73 \pm 0.57$	$+0.53 \pm 0.64$
HR 8210	21.72 ± 0.78	46 ± 2	$+80.23 \pm 0.78$	$+17.28 \pm 0.57$

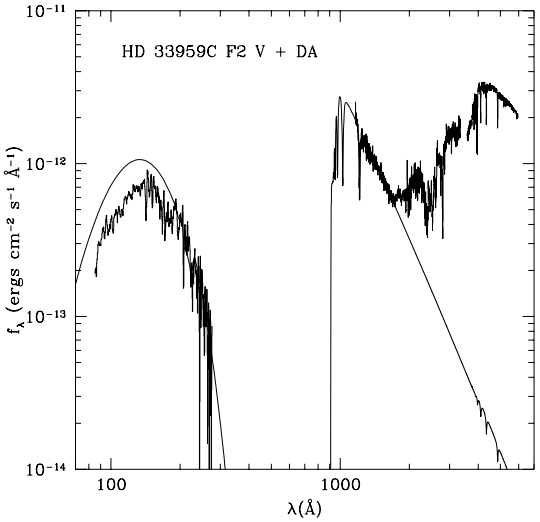

FIG. 1*e*

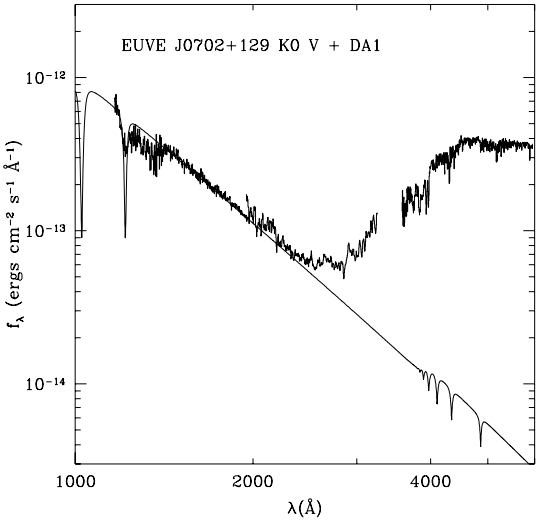

FIG. 1*f*

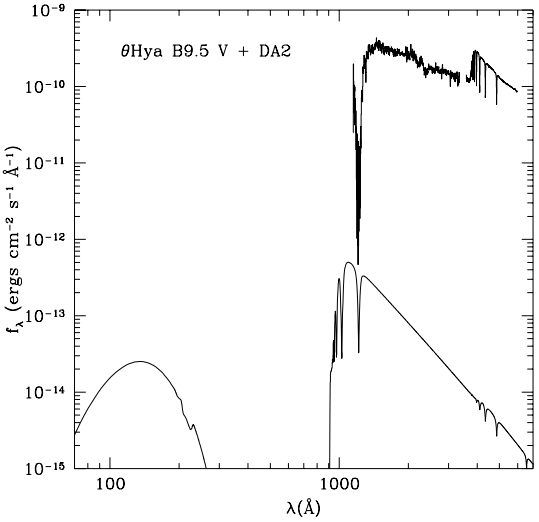

FIG. 1*g*

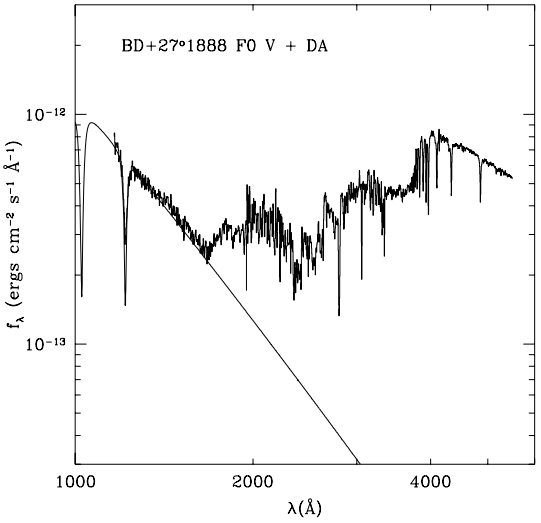

FIG. 1*h*

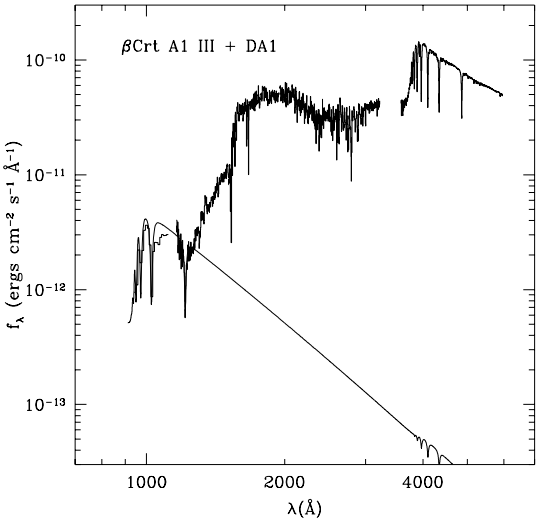

FIG. 1*i*

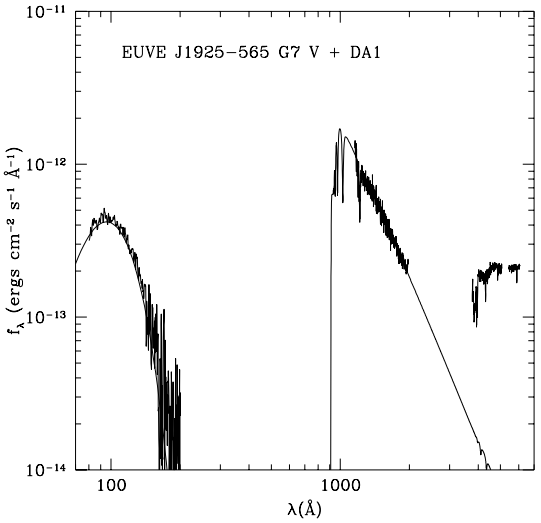

FIG. 1*j*

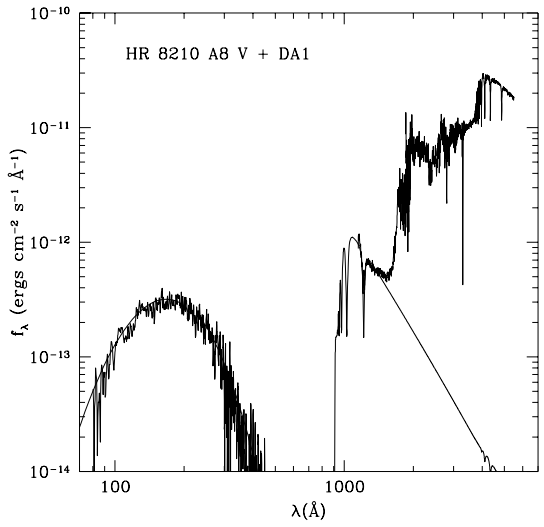

FIG. 1*k*

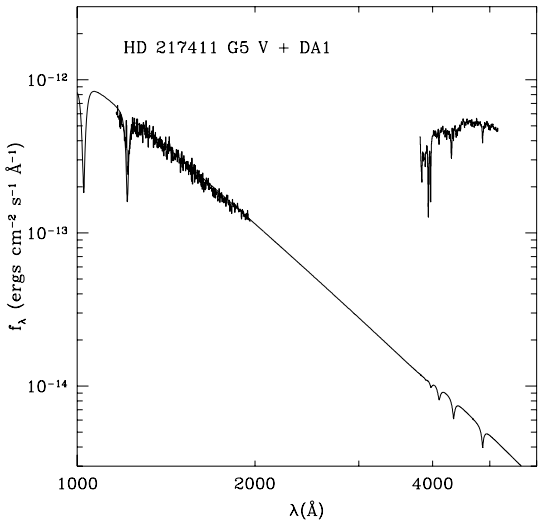

FIG. 1*l*

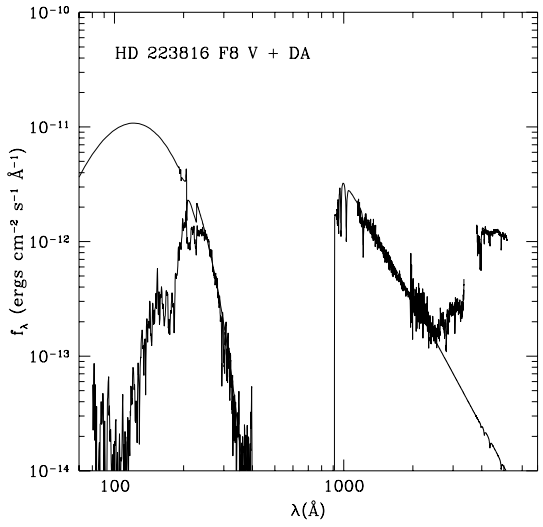

FIG. 1*m*

$i = 80 \pm 10$ km s^{-1} using the FWHM of the Ca K emission line measured in our echelle data (Fig. 2). We classified BD +08°102 as a K0 dwarf ($M_V = 5.9$) close to Kellett et al.'s classification of K2 V ($M_V = 6.5$). From its distance modulus $m_V - M_V$ (using apparent visual magnitude from Table 1), we estimate a distance of 54–71 pc. *ROSAT* measurements indicate that the K0–2 V star is an X-ray source (Table 4).

HD 15638.—(Fig. 1*b*) Landsman et al. (1993) classify this star as a F6 V ($M_V = 3.6$) in agreement with our classification. Assuming an uncertainty of two-subclass (± 0.4 mag) and a possible subgiant (F3 IV) classification ($M_V = 2.2$), as suggested in the Michigan Spectral Survey (Houk & Cowley 1975), the distance modulus results in a distance of 91–209 pc. The *Hipparcos* parallax implies a large distance (175–231 pc) that would be reconciled with the distance modulus only with a subgiant classification. High-dispersion Ca H and K spectra (Fig. 2) and *ROSAT* measurements show no evidence of emission intrinsic to the F star. Favata et al. (1995) measured the rotational velocity: $v_{\rm rot} \sin i = 62$ km s^{-1}.

HD 18131.—(Fig. 1*c*) Vennes et al. (1995) classified HD 18131 as a K0 IV star based on low-dispersion spectroscopy. We used the width of the Ca H and K emission (Montes et al. 1994) to estimate an absolute luminosity $M_V = 2.0$ (Fig. 2). This luminosity, representative of a K0 III–IV star, corresponds to a distance of 87–138 pc, somewhat larger than our earlier estimate (Vennes et al. 1995), but in agreement with the *Hipparcos* parallax. The K0 star in HD 18131 is also an 0.52–2.01 keV X-ray source (Table 4).

HR 1608.—(Fig. 1*d*) Landsman et al. (1993) critically reviewed the spectral classification of HR 1608 and assigned a K0 IV classification. Application of luminosity criteria based on Mg II and Ca II emission widths result in an absolute luminosity of $M_V = 2.1 \pm 0.4$ (Landsman et al. 1993), in agreement with our estimate based on Ca H and K emission (Fig. 2). A comparison with HD 18131 shows that the two objects are quite similar, although HR 1608 appears somewhat earlier (G5 IV). *ROSAT* measurements reveal intrinsic X-ray emission from the G–K star. Based on its absolute luminosity, we estimate the distance of HR 1608 at 38–54

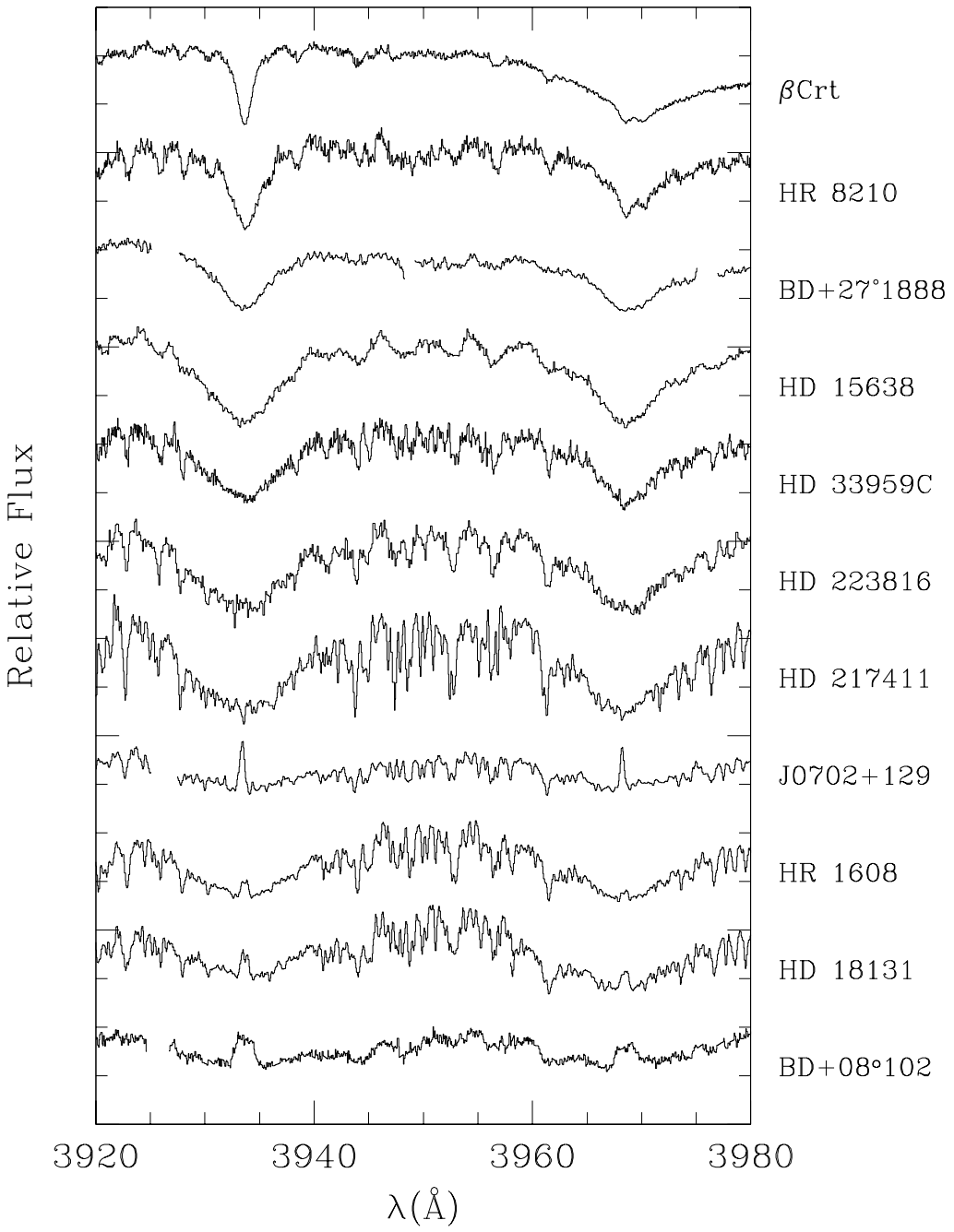

FIG. 2.—Hamilton echelle spectroscopy and MSO 74 inch coudé of the Ca H and K line profiles in selected binaries. Evidence of activity is only present in EUVE J0702+129, HR 1608, HD 18131, and BD +08°102.

pc, marginally in agreement with the *Hipparcos* data (d = 52–58 pc). Known orbital elements (§ 4) may add up to 8 mas to the apparent motion of the G–K star, which reduces confidence in the parallax and proper-motion measurements. Note that SAO and *Hipparcos* proper-motion measurements are in excellent agreement.

HD 33959C.—(Fig. 1*e*) Hodgkin et al. (1993) present optical and ultraviolet observations of the visual quadruple system HD 33959; the component A is a δ Scuti type and is a one-lined spectroscopic binary classified as A9 IV–V; the component C is classified as F3 V and is paired with a hot white dwarf companion. The companion to component A is unknown. Hodgkin et al. (1993) assign a spectral type in the range F2–6 IV–V for the C component, in agreement with our estimate of F2 V (M_V = 3.0), and derive a distance of 80–150 pc. The components A and C are possibly associated: their respective proper motions (Roeser & Bastian 1988) are close (in mas; C: $\mu_\alpha = -0.021 \pm 0.004$, $\mu_\delta = +0.003 \pm 0.004$; A: $\mu_\alpha = -0.038 \pm 0.005$, $\mu_\delta = +0.008 \pm 0.004$), but the distance moduli disagree (C: $m - M$ = 4.5–5.9; A: $m - M$ = 3.2–3.8) unless HD 33959A is reclassified as a giant. The *Hipparcos* parallax does suggest that HD 33959A is indeed quite luminous (M_V = 0.3–0.7), but unfortunately, *Hipparcos* measurements of HD 33959C appear unreliable. The orbital period of the mysterious A component is sufficiently short ($3\overset{d}{.}8$) and prospective orbital separations sufficiently close as to leave the parallax measurement unaffected. Webbink et al. (1992)

observed radial velocity variations of the F star ($P \sim 3$ days), and Tokovinin (1997) measured a relatively low rotational velocity, $v_{\rm rot} \sin i = 15.2 \pm 0.8$ km s^{-1}, corresponding to a spin period ≤ 4 days. Assuming that the F star is tidally locked to its white dwarf companion, we deduce a spin axis inclination of $i = 48°$–$63°$, adopting a radius of 1.21–1.46 $R_\odot$. The F star HD 33959C is possibly an X-ray source (Table 4), but we failed to detect Ca H and K emission in high-dispersion spectroscopy (Fig. 2).

EUVE J0702+129A.—(Fig. 1*f*) Vennes et al. (1997a) report the discovery of an active star paired with a hot white dwarf. The K0 star (hereafter EUVE J0702+129A) shows pronounced Ca H and K (Fig. 2) and Hα emission; application of the Wilson-Bappu relation (Montes et al. 1994) results in an absolute visual magnitude $M_V = 4.7 \pm 0.4$ ($m - M = 5.3 \pm 0.4$). EUVE J0702+129A lies at a distance of 95–138 pc. Narrow lines in high-dispersion optical spectroscopy limit the rotational velocity to $v_{\rm rot} \sin i \leq 5$ km s^{-1}.

θ Hya.—(Fig. 1*g*) With an assigned spectral classification between A0 V and B8 V, the detection of He I λ4471 suggests a B star classification. Bernacca & Perinotto (1970) measured a rotational velocity $v_{\rm rot} \sin i \sim 100$ km s^{-1}. The Yale General Catalogue of Trigonometric Parallaxes locates the star at a distance of 53 ± 17 pc, in agreement with *Hipparcos* measurements (38–41 pc) and the distance modulus (B9.5 V: $m - M = 3.3$), which places the star at a distance of 45 pc.

BD +27°1888.—(Fig. 1*h*) We classify the star as an F0 V, in agreement with Burleigh, Barstow, & Fleming (1997). Assuming a two-subclass uncertainty, the distance toward this object is 229–275 pc. We obtained an estimate of the rotational velocity of this F0 V star ($v_{\rm rot} \sin i = 100 \pm 10$ km s^{-1}) by convolving the F2 V spectrum of HD 33959C ($v_{\rm rot} \sin i = 15.2$ km s^{-1}) with a rotational broadening function (Gray 1976) characterized by $v_{\rm rot} \sin i = 100$ km s^{-1}.

β Crt.—(Fig. 1*i*) Fleming et al. (1991) report the discovery of this Sirius-like binary in the *ROSAT* WFC/PSPC all-sky survey. Van Altena & Sawada's (1983) trigonometric parallax would place the star at a distance of only 19 ± 4 pc, which, by inference, would suggest a F7 V classification. However, we classify β Crt as an A1 III star ($M_V = +0.1$), in agreement with Smalley et al. (1997), which places the star at a distance of 69–82 pc assuming a two subclass uncertainty. The resulting distance modulus ($m - M = 4.38$) is supported by the recent *Hipparcos* measurements, which place the star at a distance of 77–87 pc. Its projected rotational velocity ($v_{\rm rot} \sin i \sim 40$ km s^{-1}, Abt & Morrell 1995; $v_{\rm rot} \sin i \sim 47 \pm 4$ km s^{-1}, Smalley et al. 1997) is characteristic of A III–IV stars (see Abt & Morrell 1995). The discrepancy between parallax measurements may underline orbital motions.

EUVE J1925−565A.—(Fig. 1*j*) Our low-dispersion optical spectroscopy suggests a G7 V classification ($M_V = +5.4$). Again assuming a two-subclass uncertainty, the star lies at a distance of 100–120 pc. Barstow et al. (1994) report the detection of Ca H and K emission, but there is no evidence that the G7 star is an X-ray source (Table 4). The EUV/soft X-ray emission is certainly dominated by the white dwarf star.

HR 8210.—(Fig. 1*k*) Harper (1927) identified the single-line spectroscopic binary HR 8210 and measured a period of P = 21.724 days. Based on our low-dispersion spectroscopy, we classify the star as an A6 V ($M_V = +2.1$), although the star has been referred to as an A8m (see Landsman et al. 1993). Abundance studies only allow a "marginal" Am star classification (Smalley et al. 1996). Assuming a two-subclass uncertainty, the distance is 49–75 pc. The *Hipparcos* measurements are possibly affected by the orbital motion by up to 1.6 mas, i.e., twice their nominal error bars; the corrected *Hipparcos* distance is $d = 42$–50 pc, close to the distance modulus. Abt & Morrell (1995) measured a rotational velocity $v_{\rm rot} \sin i = 31$ km s^{-1}, in agreement with Smalley et al. (1996), who measured $v_{\rm rot} \sin i = 32.5 \pm 2.5$ km s^{-1}, corresponding to a rotation period of ≤ 2.3 days, revealing that the A star is not tidally locked to the white dwarf.

HD 217411.—(Fig. 1*l*) Barstow et al. (1994) report a G5 classification, in agreement with our data, and, assuming membership in the main sequence, it implies an absolute luminosity $M_V = +5.1 \pm 0.4$ or a distance of 72–105 pc. *ROSAT* measurements and a partially filled Hα line profile observed by Mullis & Bopp (1994) imply that the G star is active. Fekel (1997) measured its rotational velocity: $v_{\rm rot} \sin i = 3.4$ km s^{-1}.

HD 223816.—(Fig. 1*m*) Barstow et al. (1994) report a G0 V classification, somewhat later than our classification (F8 V), which implies an absolute luminosity $M_V = +4.0 \pm 0.2$ or a distance of 83–100 pc. *ROSAT* measurements indicate the presence of an extremely soft source, e.g., a white dwarf, and Ca H and K spectra (Fig. 2) show no evidence of emission intrinsic to the F star.

3.2. *White Dwarf Parameters*

The white dwarf parameters are obtained from an analysis of EUV and FUV continuum flux measurements, and Lyα line profiles. The quoted range of parameters are derived from 66% (1 σ), 90%, or 99% contours, as specified. The effective temperature and surface gravity measurements are converted into mass measurements using the theoretical mass-radius relations of Wood (1995) for carbon interiors without hydrogen envelopes.

Figure 3*a* shows the best fit to the FUV continuum and Lyα line profile using pure-hydrogen models, and Figure 3*b* (*thin full lines*) shows the corresponding confidence contours in the $T_{\rm eff}$ and log g plane at 66% (1 σ), 90%, and 99%. Although the 66% contours sometimes favor a high or a low gravity, the 99% contours allow a broader range of solutions, often confined to a band in the $T_{\rm eff}$ and log g plane. For a given $T_{\rm eff}$ and log g, we then evaluate the projected apparent visual magnitude (m_V) based on the FUV model fit, and we compute the absolute visual magnitude (M_V) using the evolutionary mass-radius relations of Wood (1995). We finally estimate a distance from the distance modulus.

Figure 3*b* also shows the allowed range of distances, based either on the luminosity (*dashed*) or on the parallax (*thick full lines*), toward the secondary stars as determined in § 3.1. Overlap between the two areas, one delimited by the white dwarf parameters and the other by the secondary star parameters, defines the most probable set of parameters for the white dwarf, *assuming* a physical association between the white dwarf and the luminous star.

Figures 4*a*–4*d* show the best fit to the EUV continuum, again using pure-hydrogen model atmospheres, for HD 15638, HD 33959C, EUVE J1925–565B, and HR 8210. Best solutions are searched for in the ($T_{\rm eff}$, g, $n_{\rm H}$) parameter space, and 66% (1 σ), 90%, and 99% confidence contours are projected on the ($T_{\rm eff}$, log $n_{\rm H}$)- and ($T_{\rm eff}$, log g)-planes.

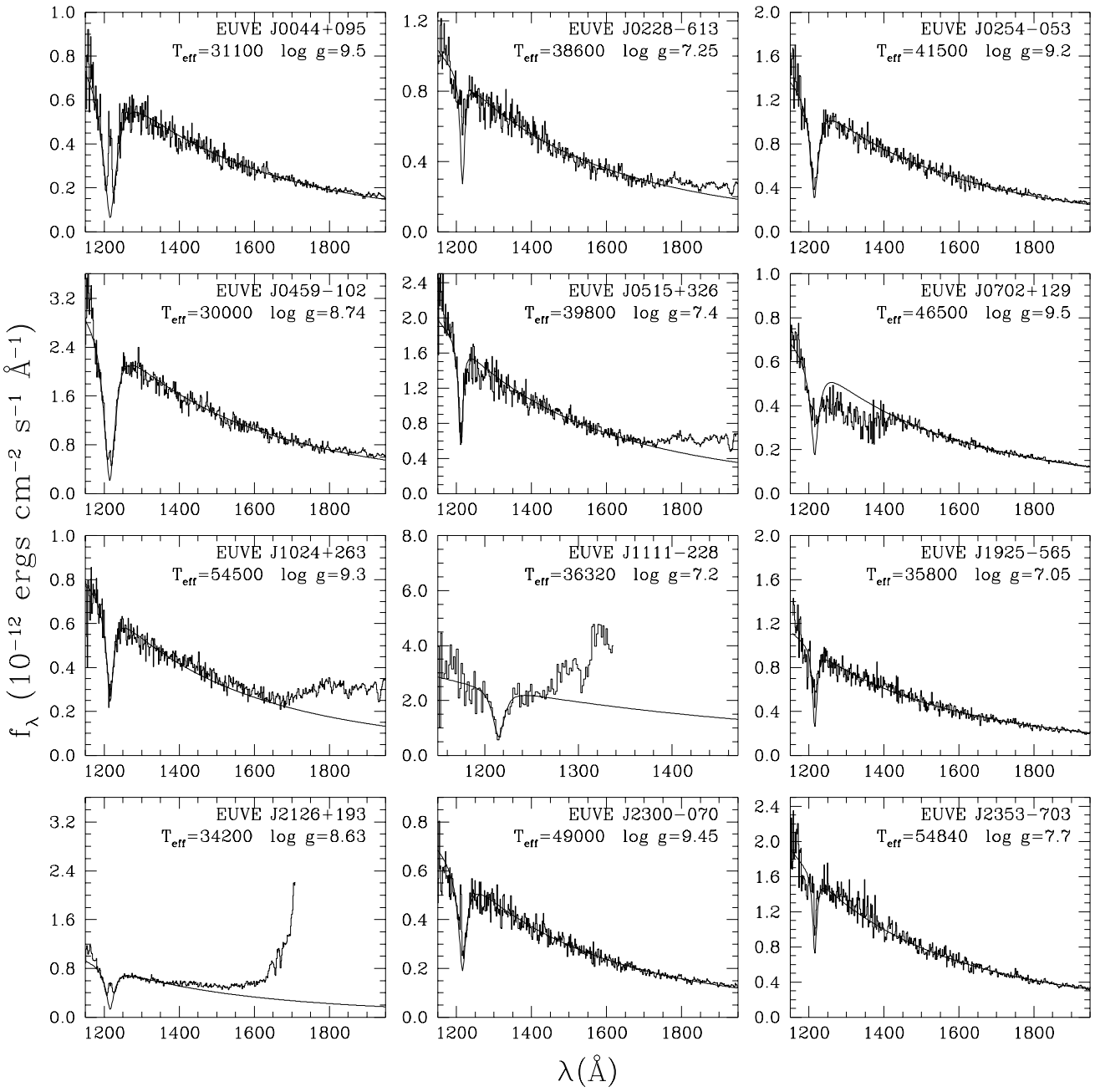

FIG. 3*a*

FIG. 3.—(*a*) Model atmosphere analysis of the FUV energy distributions of white dwarfs in selected binaries. We present the *IUE* SWP spectra and best model fits adopting a pure-hydrogen composition. Note that wide ranges of solutions are acceptable (Table 7; *b*). The fits are restricted to a wavelength range dominated by the white dwarf. (*b*) Confidence contours (*full thin lines*) of the FUV model atmosphere fit at 66%, 90%, and 99% in the ($T_{\rm eff}$, log *g*)-plane and ranges of distances adopted for the secondary star based on the distance modulus (*dashed lines*) and the *Hipparcos* parallax (*full thick lines*). Assuming a physical association between the white dwarf and its companion helps constrain the white dwarf parameters (§ 3.2).

Each model is normalized to the measured flux at 1300 Å and attenuated by interstellar absorption assuming the column density ratios He I/H I = 0.07 and He II/H I = 0.03. Figure 5 shows the EUV (*EUVE*, *ROSAT* WFC) and soft X-ray (PSPC 0.1–0.4 keV) count rate analyses for the remaining white dwarfs; uncertain count rates are treated as upper limits. We adopted a minimum count rate uncertainty of ±25%; finally, we excluded the *ROSAT* PSPC count rate if a detection also occurred in the 0.5–2.0 keV band. The data were analyzed with the same normalization procedure and ISM model adopted in the EUV spectral analyses. Photometric data are less sensitive than spectroscopic data to surface gravity (which we allow to vary between log g = 7.0 and 9.5) and to the presence of heavy elements, and, in general, provide less accurate $T_{\rm eff}$ or log $n_{\rm H}$ determinations.

We now examine individual white dwarf properties.

EUVE J0044+095.—(Companion of BD +08°102; Figs. 3 and 5) A joint analysis of the *IUE* Lyα and FUV continuum and the EUV photometric data suggests a high

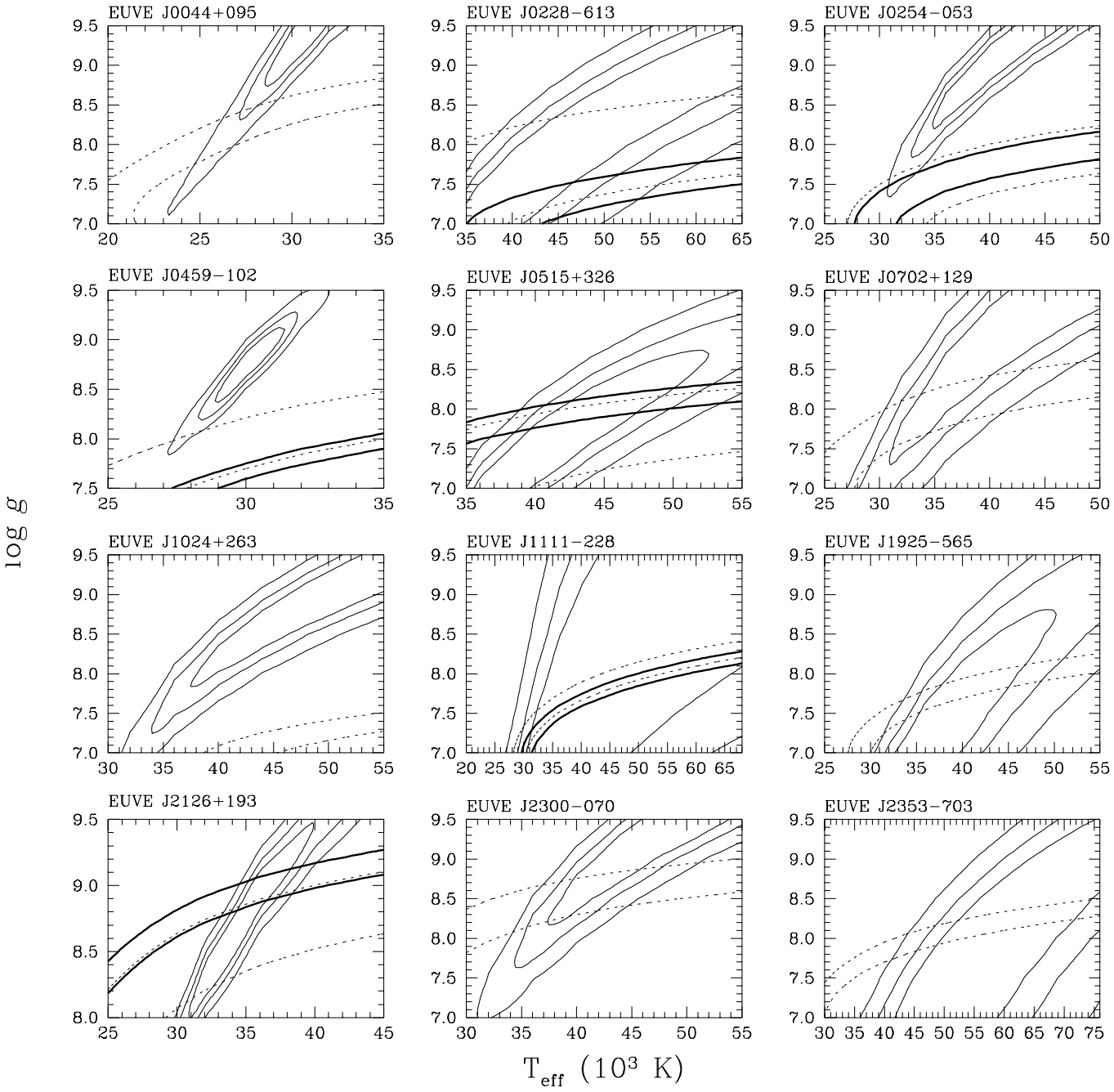

FIG. 3*b*

white dwarf surface gravity ($8.5 \leq \log g \leq 9.5$) and a temperature between 28.0 and 32.0 $\times$ 10^3 K (90% contours). These parameters are marginally consistent (99% contours), in the lower range, with parameters corresponding to the secondary's distance ($m - M = 3.7$–4.3): $T_{\rm eff} = (25$–$28) \times 10^3$ K and $\log g = 7.8$–8.5. Using Wood's (1995) mass-radius relations, the white dwarf mass covers a wide range (0.50–1.35 $M_\odot$), most likely near 0.92 $M_\odot$ ($\log g = 8.5$, $T_{\rm eff} = 28{,}000$ K). Assuming a pure-hydrogen white dwarf atmosphere, we infer a neutral hydrogen column density $n_{\rm H\,I} = (2$–$4) \times 10^{19}$ cm^{-2}.

EUVE J0228−613.—(Companion of HD 15638; Figs. 3 and 4*a*) A joint analysis of FUV and EUV spectroscopic measurements independently constrains the effective temperature and surface gravity to $T_{\rm eff} = (45.0$–$49.5) \times 10^3$ K and $\log g = 7.5$–8.8 (90%). The parameters imply a distance of 73–156 pc, in agreement with our estimate of the distance toward the F star companion (91–209 pc; § 3.1). The *Hipparcos* parallax implies a larger distance and may be affected by systematic uncertainties caused by orbital motion. The white dwarf mass is 0.44–1.10 $M_\odot$. The EUV spectrum reveals a white dwarf atmosphere possibly pure in hydrogen; the measured neutral hydrogen column density is $n_{\rm H\,I} = (2.0$–$2.4) \times 10^{19}$ cm^{-2}.

EUVE J0254−053.—(Companion of HD 18131; Figs. 3 and 5) Assuming a pure hydrogen atmosphere, the EUV photometric data and the *IUE* Lyα and FUV continuum measurements constrain the temperature and gravity to

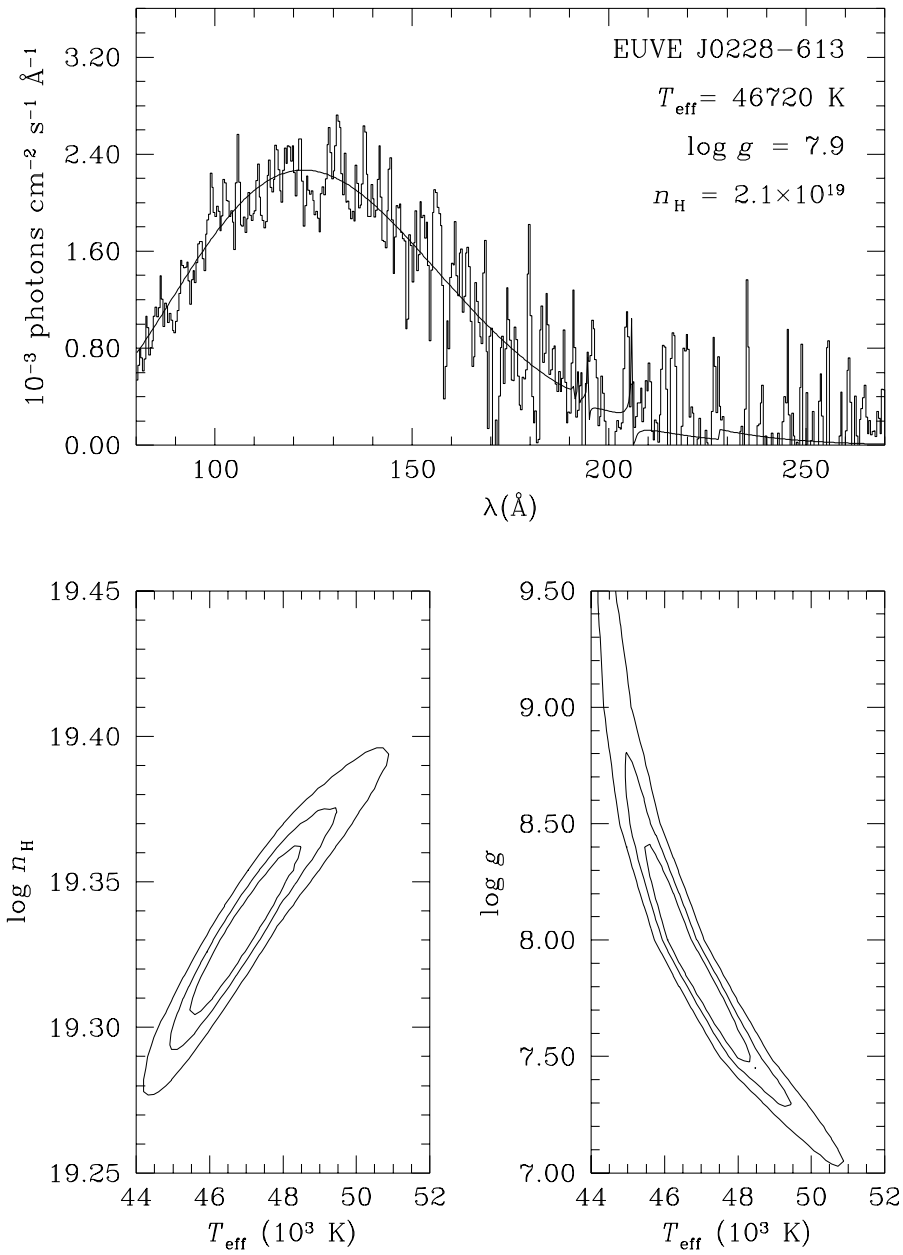

FIG. 4*a*

FIG. 4.—(*a*) Model atmosphere analysis of the EUV energy distribution of the white dwarf in EUVE J0228−613 (HD 15638). *Top: EUVE* spectra (SW + MW) and the best model fit adopting a pure-hydrogen composition. *Bottom:* Confidence contours at 66%, 90%, and 99% in the ($T_{\rm eff}$, g)- and ($T_{\rm eff}$, $n_{\rm H}^{\rm ISM}$)-planes. (*b*) As (*a*), but for EUVE J0515+323 (HD 33959C). Heavy-element opacities are evident at shorter wavelength, and the fit is restricted to $\lambda > 190$ Å. (*c*) As (*a*), but for EUVE J1925−565B. (*d*) As (*a*), but for EUVE J2126+193 (HR 8210). (*e*) Comparative study of EUVE J2353−703 (HD 223816) and the known isolated DA white dwarfs G191-B2B and MCT 0455−2812 (see discussion in § 3.2).

$T_{\rm eff}$ = (33.0–43.0) × 10^3 K and log $g \geq$ 7.9 (90%). However, at the secondary's distance ($m - M$ = 4.7–5.7), the white dwarf surface gravity is limited to log $g \leq$ 7.8. The parameters are possibly close to $T_{\rm eff}$ = (33.0–34.0) × 10^3 K and log g = 7.7–7.8, implying a mass of ∼0.48–0.52 $M_\odot$. With these parameters the neutral hydrogen column density is $n_{\rm H\,I}$ = (2.0–4.0) × 10^{19} cm^{-2}.

EUVE J0459−102.—(Companion of HR 1608; Figs. 3 and 5) *IUE* Lyα and continuum measurements favor a high-gravity log g = 8.2–9.3 (90%). The high luminosity of the secondary star HR 1608 places the system at a distance $d \geq$ 38 pc, implying a lower surface gravity (log $g \leq$ 8.1), outside the 90% confidence range of the spectroscopic measurements. The most likely parameters are $T_{\rm eff}$ = (27.0–28.7) × 10^3 K and log g = 7.8–8.1, i.e., M = 0.51–0.67 $M_\odot$. The white dwarf parameters and *Hipparcos* parallax are mutually exclusive, which either proves that the two objects (G–K star and white dwarf) are unrelated or, most likely, that the parallax measurement is definitely affected by the orbital motion (see § 3.1). EUV photometric measurements limit the neutral hydrogen column density in the local ISM to $n_{\rm H} \leq 2 \times 10^{19}$ cm^{-2}.

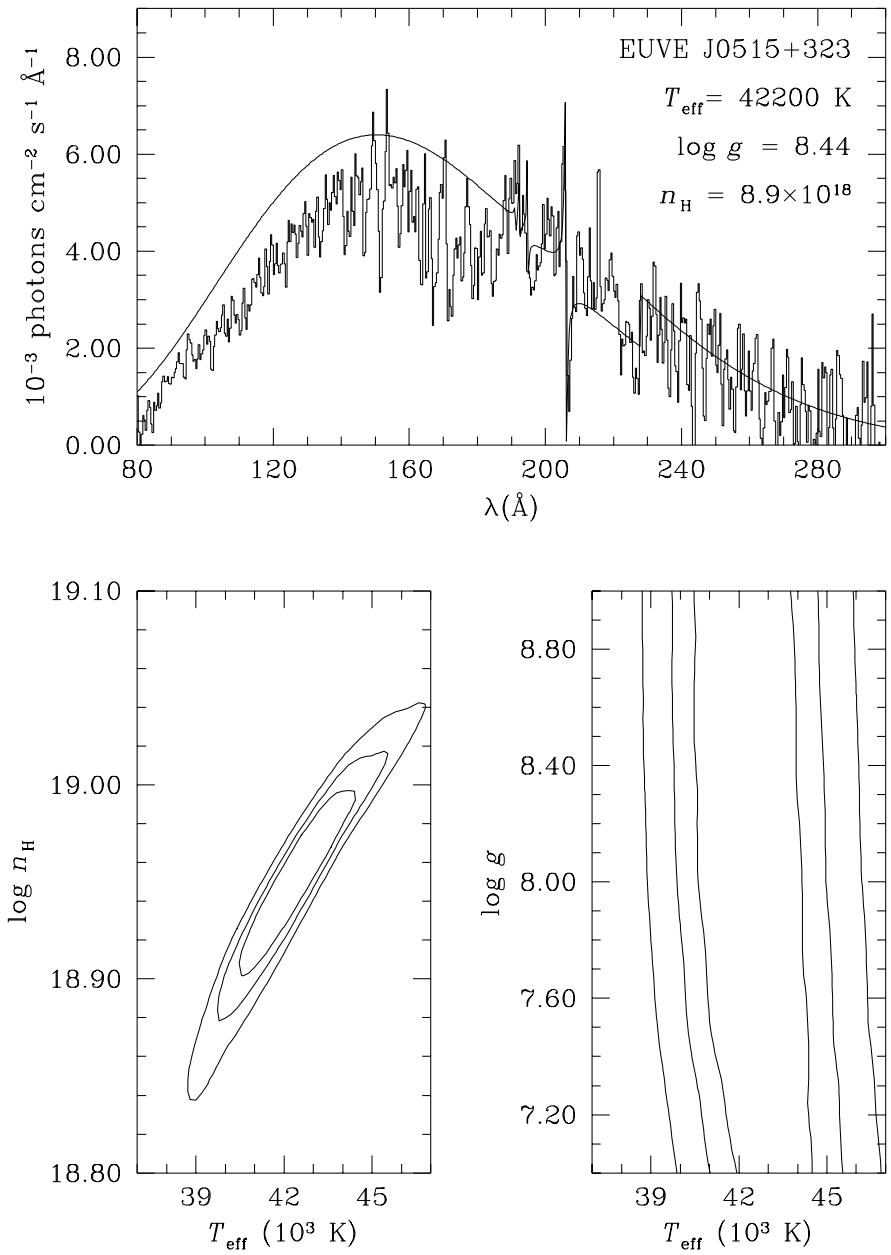

FIG. 4*b*

EUVE J0515+326.—(Companion of HD 33959C; Figs. 3 and 4*b*) An analysis of the joint FUV and EUV continuum spectrum limits the temperature and surface gravity to $T_{\rm eff} = (40.5–45.0) \times 10^3$ K and log $g = 7.0–8.5$ (90%). Figure 4*b* shows a close correspondence between the observation and a pure hydrogen model at $\lambda \geq 190$ Å, while the observation shows evidence of trace opacities below 190 Å. The neutral hydrogen column density is $n_{\rm H\,I} = (0.8–1.0) \times 10^{19}$ cm^{-2}. A physical association with HD 33959C also limits the surface gravity to log $g = 7.1–8.1$. The inferred mass is $\sim$0.30–0.69 $M_\odot$. Adopting instead the distance toward HD 33959A, which is likely associated with HD 33959C, the white dwarf parameters are restricted to $T_{\rm eff} = (40.5–45.0) \times 10^3$ K and log $g = 7.8–8.1$. The white dwarf mass is further constrained to 0.53–0.69 $M_\odot$.

EUVE J0702+129B.—(Figs. 3 and 5) The *IUE* spectra and EUV photometric measurements limit the temperature to $T_{\rm eff} = (28–50) \times 10^3$ K, but the surface gravity remains unconstrained (90%). However, at the distance of the K0 companion the surface gravity is constrained to log $g =$ 7.3–8.5 and the temperature to $T_{\rm eff} = (29.0–43.0) \times 10^3$ K. Adopting these parameters, the inferred mass is $\sim$0.32–0.93 $M_\odot$, and the neutral hydrogen column density is constrained by EUV photometric measurements to $n_{\rm H\,I} = (0.4–6.0) \times 10^{19}$ cm^{-2}.

EUVE J0914+023.—(Companion of θ Hya; Fig. 5) The presence of a white dwarf companion to the B9.5 V star θ Hya is not immediately evident. Figure 1*g* shows the B star with a plausible white dwarf companion at a distance of 50 pc. EUV spectroscopic observations are the only available means to identify the white dwarf unambiguously. The *ROSAT* X-ray measurements reveal an extremely soft source, characteristic of a hot white dwarf star, and the EUV measurements are consistent with a white dwarf tem-

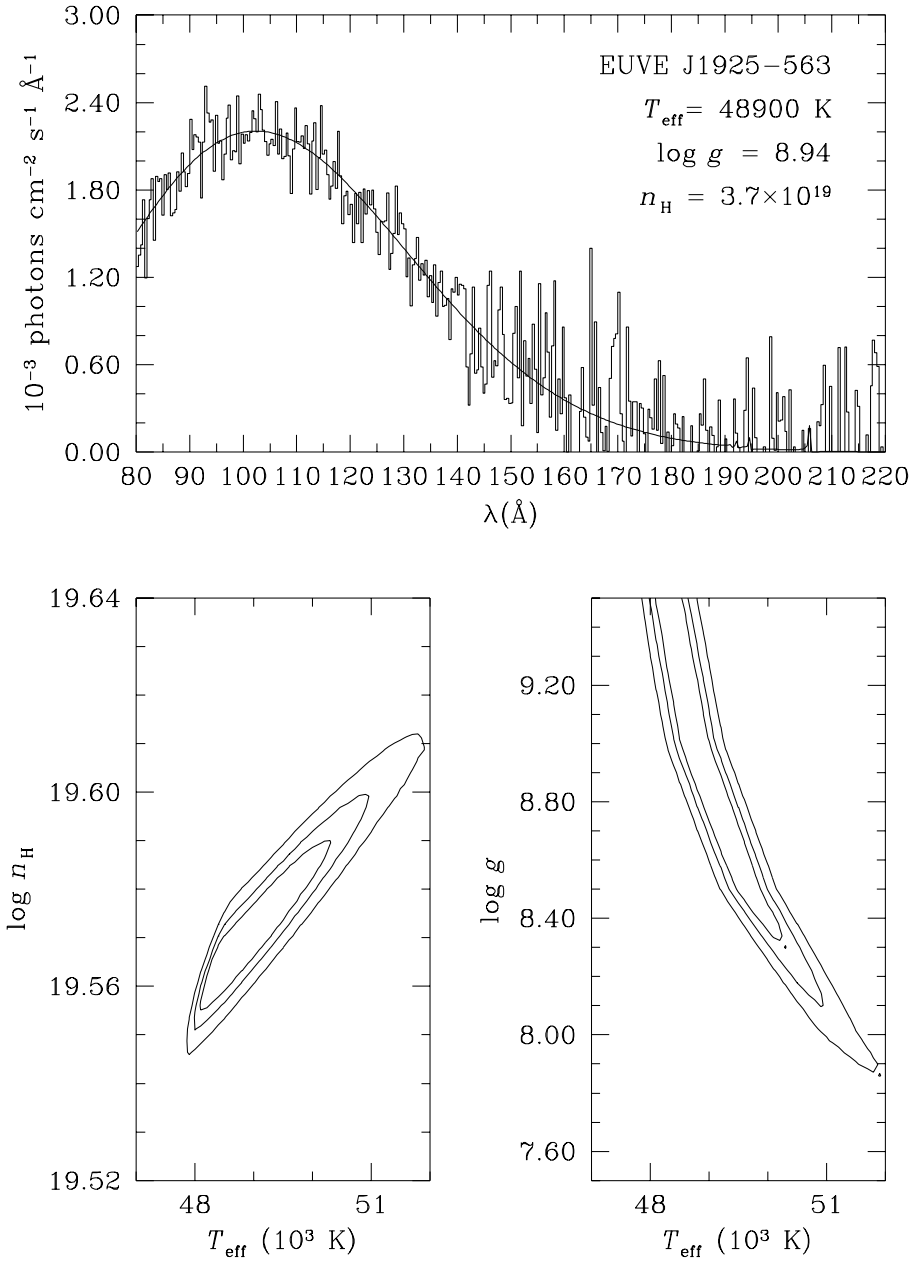

FIG. 4*c*

perature of $T_{\rm eff} = (28.7–32.7) \times 10^3$ K (assuming log g = 9.0) and neutral hydrogen column density $n_{\rm H\,I} \leq 6 \times 10^{18}$ cm^{-2} (90%). Although the surface gravity cannot be estimated directly based on photometric measurements, it is presumed that a star earlier than B9.5 ($\geq 3.3\ M_\odot$) is a likely progenitor of a massive white dwarf. Forthcoming EUV spectroscopic data will constrain the effective temperature and, indirectly, the surface gravity (and mass).

EUVE J1024+263.—(Companion of BD +27°1888; Figs. 3 and 5) The F0 V star and the white dwarf form an unlikely pair. The effective temperature and surface gravity of the white dwarf are constrained to $T_{\rm eff} = (34.0–40.0) \times 10^3$ K and log g = 7.3–8.5 (90%), imposing a distance $d \leq 171$ pc. Unless the F0 V star is dramatically underluminous, it is possibly at a much larger distance (229–275 pc) than the white dwarf itself. This pair of objects is at high Galactic latitude, and a chance alignment also appears unlikely. The white dwarf mass is 0.34–0.93 $M_\odot$, and EUV/soft X-ray photometric measurements constrain the neutral hydrogen column density in the local ISM to $n_{\rm H\,I} = (4.0–7.0) \times 10^{19}$ cm^{-2}. In summary, in-depth analysis of the white dwarf and F0 V stellar parameters using additional FUV and high-resolution optical data is required.

EUVE J1111−228.—(Companion of β Crt; Figs. 3 and 5) The giant A star dominates the optical and ultraviolet emission, but a narrow window ($\lambda \leq 1250$ Å) remains uncontaminated. The fit to the Lyα line profile only weakly constrains the stellar parameters, but assuming a pure hydrogen atmosphere, the EUV photometric measurements and FUV data limit the white dwarf temperature to $T_{\rm eff} = (29.0–33.0) \times 10^3$ K and the surface gravity to log $g \leq 8.3$ (90%). At the companion's distance the surface gravity is

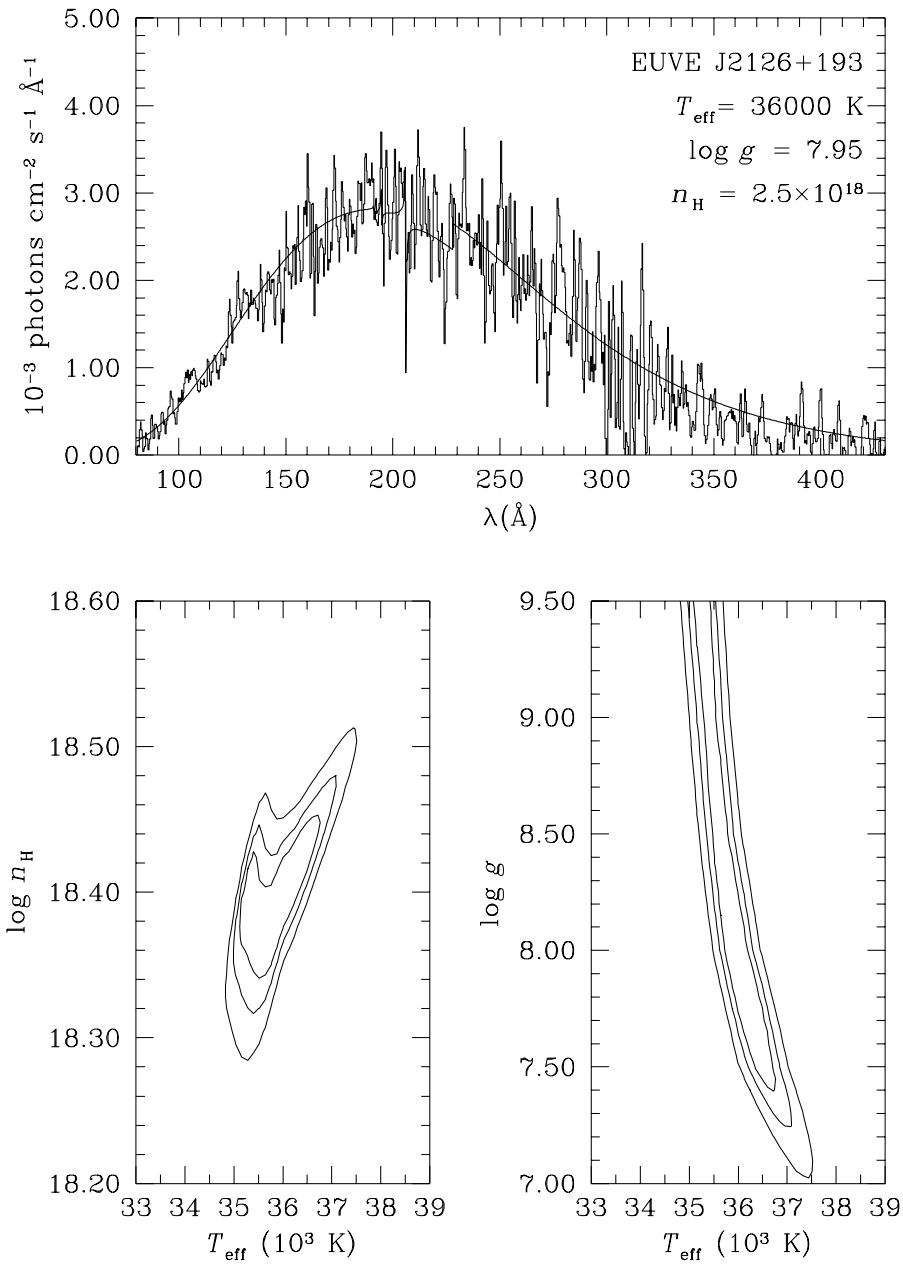

FIG. 4*d*

further constrained to log $g \leq 7.6$, implying a low-mass white dwarf ($M = 0.44\ M_\odot$). The neutral hydrogen column density in the ISM is $n_{\rm H\,I} = (0.7\text{–}2.0) \times 10^{19}$ cm^{-2}. Clearly, new EUV and FUV spectroscopic measurements will greatly improve our knowledge of this white dwarf.

EUVE J1925−565B.—(Figs. 3 and 4*c*) The strong EUV continuum emission was measured with *EUVE* and constrains the atmospheric parameters: $T_{\rm eff} = (48.0\text{–}51.0) \times 10^3$ K and log $g \geq 8.1$ (90%). The atmosphere is possibly pure in hydrogen, and the neutral hydrogen column density in the ISM is $n_{\rm H\,I} = (3.5\text{–}4.0) \times 10^{19}$ cm^{-2}. Lyα is only weakly detected and limits the surface gravity to log $g \leq 9.2$ (90%). The parameters are marginally consistent with the G7 V distance, which implies log $g = 8.1\text{–}8.2$ (at $T_{\rm eff} =$ 50,000 K) and a white dwarf mass of 0.70–0.76 $M_\odot$.

EUVE J2126+193.—(Companion of HR 8210; Figs. 3 and 4*d*) Early estimates of the mass function of this binary already required a massive ($M \geq 1.1\ M_\odot$) and underluminous companion to the A star (Harper 1927). The analysis of the EUV continuum and FUV Lyα measurements are consistent with $T_{\rm eff} = (35.5\text{–}36.0) \times 10^3$ K and log $g = 8.6\text{–}9.2$ (99%), corresponding to $M = 1.00\text{–}1.32\ M_\odot$. At the 99% level, the surface gravity can be as high as 9.2, corresponding to a mass of 1.32 $M_\odot$, but at the distance set by the *Hipparcos* parallax, the parameters of the white dwarf are $T_{\rm eff} = 35{,}200\text{–}35{,}500$ K and log $g = 8.85\text{–}9.05$, or a mass of 1.13–1.24 $M_\odot$. A comparison with an accurate mass function is presented in § 4. The EUV spectra constrain the neutral hydrogen column density in the local ISM to $n_{\rm H\,I} = (2.2\text{–}2.8) \times 10^{18}$ cm^{-2}.

EUVE J2300−070.—(Companion of HD 217411; Figs. 3 and 5) The *IUE* FUV continuum and Lyα data limit the white dwarf parameter to $T_{\rm eff} \geq 34{,}000$ K and log $g \geq 7.6$ (90%). At the distance of the G5 V star, the parameters of

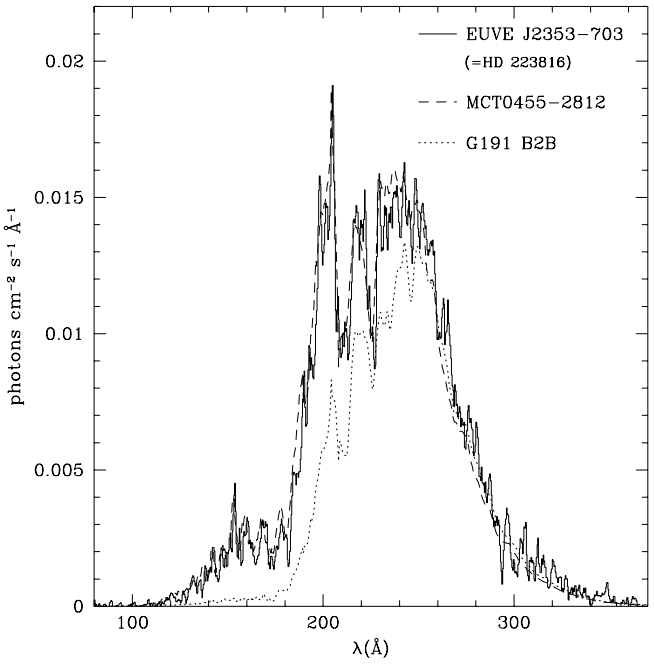

FIG. 4*e*

the white dwarf are $T_{\rm eff} = (35.5–47.0) \times 10^3$ K and log $g = 8.1–8.9$, i.e., $M = 0.68–1.16\ M_\odot$. The EUV photometric measurements imply a relatively high neutral hydrogen column density in the local ISM of $n_{\rm H\,I} = (3.0–8.0) \times 10^{19}$ cm^{-2}.

EUVE J2353−703.—(Companion of HD 223816; Figs. 3 and 4*e*) The white dwarf in the binary HD 223816 shows weak Lyα absorption, from which we derive $T_{\rm eff} = (49–74) \times 10^3$ K and log $g = 7.9–8.5$ at the F8 V distance (66%), implying a mass of 0.60–0.95 $M_\odot$. The white dwarf in HD 223816 may well have the highest temperature of the sample, as revealed by the *EUVE* spectra. Figure 4*e* shows a comparison between *modified* spectra of the two hot DA white dwarfs G191-B2B and MCT 0455−2812 (Dupuis et al. 1995), and the white dwarf in HD 223816. The spectra of G191-B2B and MCT 0455−2812 were modified to match the shape of the EUV spectrum of EUVE J2353−703 between 250 and 350 Å by including the effect of larger H I column densities in the local ISM and a correction to the solid angle subtended by the star. We folded G191-B2B's spectrum ($n_{\rm H\,I} = 2 \times 10^{18}$ cm^{-2}, $T_{\rm eff} = 54{,}000$ K; Dupuis et al. 1995) with an additional H I column of 9×10^{18} cm^{-2}, resulting in a total column of $n_{\rm H\,I} = 1.1 \times 10^{19}$ cm^{-2}, and the spectrum was scaled down by a factor of 0.375. Similarly we folded MCT 0455−2812's spectrum ($n_{\rm H\,I} = 1 \times 10^{18}$ cm^{-2}, $T_{\rm eff} = 64{,}000$K; Dupuis et al. 1995) with an additional column of 1.0×10^{19} cm^{-2}, again resulting in a total column of $n_{\rm H\,I} = 1.1 \times 10^{19}$ cm^{-2}, and the spectrum was scaled up by a factor of 1.5. A comparison between these objects shows that EUVE J2353−703 and MCT 0455−2812 are EUV spectroscopic twins. Assuming, to first approximation, that all three objects have identical stellar parameters, we estimate the visual magnitude of EUVE J2353−703 as $V = 13.56$ or 12.84 when scaled on MCT 0455−2812 or G191-B2B, respectively. A comparison with the FUV-projected optical magnitude (14.0–14.2) suggests that EUVE J2353−703 is actually much hotter than G191-B2B and only slightly hotter than MCT 0455−2812: applying a model atmosphere analysis to the EUV/FUV flux ratios results in differential temperatures of $T - T_{\rm MCT} = +5000$ K and $T - T_{\rm G191\text{-}B2B} = +15{,}000$ K. Therefore, the parameters of EUVE J2353−703 are possibly close to $T_{\rm eff} \sim 70{,}000$ K and log $g = 8.2–8.5$. The atmospheric chemical composition of EUVE J2353−703 is possibly identical to the composition of MCT 0455−2812; Vennes et al. (1996b) measured a silicon abundance of Si/H = (1–3) $\times 10^{-6}$ and a phosphorus abundance of P/H = (2–3) $\times 10^{-8}$ in FUV spectra of MCT 0455−2812. A similar heavy-element abundance is likely to be present in EUVE J2353−703 as well.

Table 7 summarizes our temperature and gravity measurements based on FUV and EUV data. Table 7 also compares our results to other published FUV measurements. The comparison reveals some discrepancies at high temperatures, but, in general, shows agreement between measurements. However, neither the mass nor the chemical composition of these white dwarfs is firmly established; the white dwarf parameters are sometimes marginally consistent with distance estimates toward the companion star. Moreover, the dominant uncertainty, i.e., the existence of a 99% solution in temperature for any given surface gravity ($7.0 \leq \log g \leq 9.5$), can only be alleviated with spectroscopic measurements of the complete Lyman line series that offer a detailed effective temperature versus surface gravity diagnostic (see Vennes et al. 1996b).

4. ORBITAL PARAMETERS

We measured the wavelength centroid of the Hα ($\lambda = 6562.80$) absorption core in a sample of 13 objects. Strong Hα emission precluded such measurements in EUVE J0702+129 (Vennes et al. 1997a), and we instead used the Fe I λ6592.92 triplet. The K2 V BD +08°102 and the early-type stars BD +27°1888 and θ Hya have high rotational velocities that do not allow accurate radial velocity measurements. The measurements were converted to velocities and transformed into the barycentric reference frame. Table 8 presents the log of observations and radial velocity measurements: columns (1) and (4) list the observation dates (UT), and columns (2) and (5) list the mid-exposure heliocentric Julian dates. Finally, columns (3) and (6) list the barycentric-corrected radial velocities. We monitored a number of radial velocity standards (HD 22484, HD 102870, HD 112299, HD 136202, HD 154417, HD 187691, and HD 222368; Astronomical Almanac 1995), and we achieved in most cases an accuracy of $\Delta v = \pm 1$ km s^{-1}. This accuracy degraded in measurements of the fast-rotating BD +27°1888 and θ Hya (approximately $\Delta v = \pm 5$ km s^{-1}).

Mass functions are determined from

$$f(m) = \frac{M_1^3 \sin^3 i}{(M_1 + M_2)^2} = (1 - e^2)^{3/2} \frac{PK_2^3}{2\pi G}\,, \qquad (1)$$

where M_1 is the mass of the white dwarf, M_2 is the mass of the secondary, P is the orbital period, e is the eccentricity, i is the orbital inclination, and K_2 is the secondary orbital velocity.

We now examine orbital properties of the systems in our sample.

BD +08°102.—Kellett et al. (1995) found no radial velocity variations on a timescale of several days ($v_{\rm rad} = 24.0$

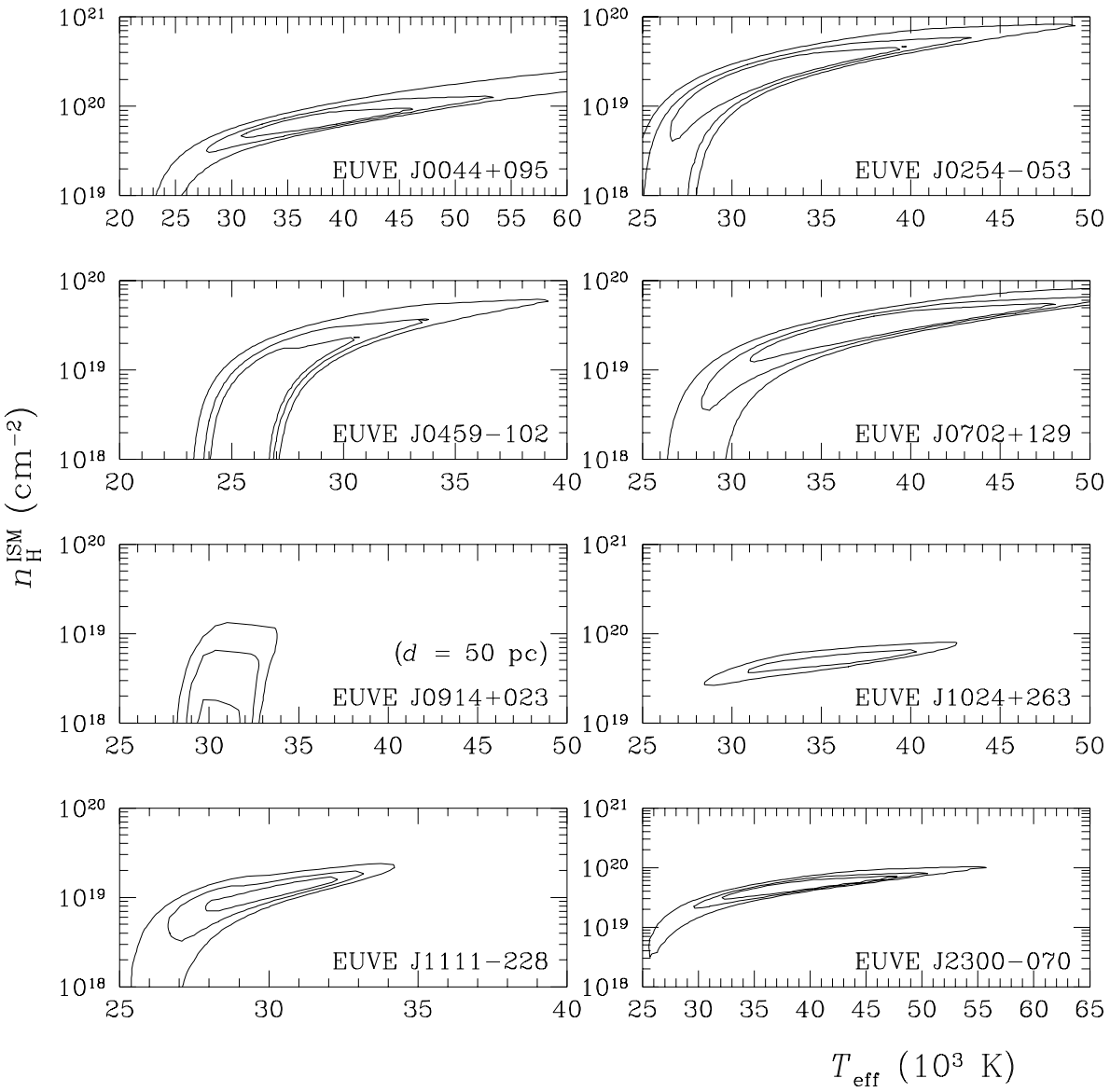

FIG. 5.—Model atmosphere analysis of EUV photometric measurements (*EUVE*, *ROSAT* WFC) for the white dwarfs in selected binaries

$\pm$ 1.5 km s^{-1}). Low-S/N spectra obtained with the Lick coudé auxiliary telescope did not allow us to obtain useful measurements. New high-S/N observations of this object are planned for 1998–1999 at the MSO 74 inch telescope.

HD 15638.—(Table 8) A short series of four measurements obtained on three nights show a constant radial velocity with an average of -0.7 km s^{-1} and a standard deviation of 0.7 km s^{-1}.

HD 18131.—(Table 8; Fig. 9) Vennes et al. (1995) could not place a useful limit on radial velocity variations of the K0 star ($K \leq 30$ km s^{-1}). Our high-dispersion data apparently indicate variations of the order of a few kilometers per second on a 1 yr timescale. The average velocity is $+18.0$ km s^{-1} with a standard deviation of 1.9 km s^{-1}.

HR 1608.—(Table 8; Fig. 10) Beavers & Eitter (1988) measured the orbital elements of this single-line spectroscopic binary. Adopting a period of 903 days, an eccentricity of 0.3, and adjusting the pericenter epoch ($T_0 =$ 24,500,384 $\pm$ 51) and periastron position ($\omega = 171° \pm 22°$), we determined a systemic and orbital velocity (K) of -14.8 and 4.8 km s^{-1}, respectively, in agreement with Beavers & Eitter (1988; $K = 5.0 \pm 0.3$). The mass of the K0/G5 subgiant is uncertain, possibly larger than 1.5 $M_\odot$; the mass function then implies a minimum mass of 0.27 $M_\odot$.

HD 33959.—(Table 8; Figs. 6, 11, and 12) Our radial velocity measurements suggest a physical association between the components A and C, although proper-motion measurements marginally differ, and the distance moduli disagree (§ 3.1). Tokovinin (1997) independently derived the orbital elements of HD 33959C (ADS 3824C) in agreement with our measurements. Combining Tokovinin's data with our data doubles the time base and considerably refines the period measurement, $P = 2.99322 \pm 0.00005$ days (Table 9). The clustering of data in phase is due to the fact that the period is 3.0013 sidereal days. However, the precision of individual measurements is such that there is no possibility of cycle count errors. Based on our data we determine an accurate mass function that limits the mass of the white dwarf to $M \geq 0.25\ M_\odot$. If we assume that the F star spin axis is normal to the orbital plane ($i = 48°$–$63°$; § 3.1), the

TABLE 7

WHITE DWARF PROPERTIES

	FUV			EUV		FUV OTHER WORK	
NAME	log g	$T_{\rm eff}$ (10^3 K)	d (pc)	$T_{\rm eff}$ (10^3 K)	Notes	$T_{\rm eff}$ (10^3 K)	References
EUVE J0044+095.....	9.5	31.1	26	28.0–53.0	Photometry	...	
	9.0	29.5	37	28.0–53.0	log g = 7.0–9.5	29.9	B94
	8.5	27.8	52	28.0–53.0		28.3	B94
	8.0	26.0	66	28.0–53.0		26.6	B94
	7.5	24.5	82	28.0–53.0		24.9	B94
EUVE J0228−613.....	9.5	65.0	41	...		...	
	9.0	60.8	63	...		63.1, 58.9	L93, B94
	8.5	52.4	89	~45.5	Spectroscopy	54.5, 54.8	L93, B94
	8.0	45.8	120	~46.5		47.6, 51.7	L93, B94
	7.5	40.4	156	~48.0		41.9, 47.2	L93, B94
	7.0	36.2	185	...		37.3, 44.0	L93, B94
EUVE J0254−053.....	9.5	44.0	27	25.0–43.0	Photometry	...	
	9.0	40.0	40	25.0–43.0	log g = 7.0–9.5	35.1	B97
	8.5	36.5	58	25.0–43.0		33.0	B97
	8.0	34.0	77	25.0–43.0		31.1	B97
	7.5	31.5	99	25.0–43.0		29.3	B97
EUVE J0459−102.....	9.5	32.8	14	24.0–34.0	Photometry	...	
	9.0	31.0	21	24.0–34.0	log g = 7.0–9.5	31.6, 30.5	L93, B94
	8.5	29.4	30	24.0–34.0		29.5, 28.8	L93, B94
	8.0	27.8	38	24.0–34.0		27.6, 27.3	L93, B94
EUVE J0515+326.....	9.0	55.0	42	40.5–43.8	Spectroscopy	55.8	B94
	8.5	49.4	62	40.5–44.0		51.5	B94
	8.0	44.6	84	40.7–44.0		46.6	B94
	7.5	40.6	113	41.0–44.3		42.3	B94
	7.0	37.4	139	42.0–44.5		40.1	B94
EUVE J0702+129.....	9.5	46.5	40	28.0–50.0	Photometry	...	
	9.0	41.5	59	28.0–50.0	log g = 7.0–9.5	...	
	8.5	37.5	84	28.0–50.0		...	
	8.0	34.5	112	28.0–50.0		...	
	7.5	32.0	144	28.0–50.0		...	
	7.0	29.5	157	28.0–50.0		...	
EUVE J1024+262.....	9.5	57.5	43	31.0–40.0	Photometry	...	
	9.0	50.0	64	31.0–40.0	log g = 7.0–9.5	47.6	B97
	8.5	43.5	90	31.0–40.0		42.5	B97
	8.0	39.0	120	31.0–40.0		38.4	B97
	7.5	35.5	156	31.0–40.0		35.4	B97
	7.0	32.5	178	31.0–40.0		33.2	B97
EUVE J1111−228.....	9.5	60.3	23	26.5–33.0	Photometry	...	
	9.0	53.6	35	26.5–33.0	log g = 7.0–9.5	43.8	B94
	8.5	47.8	50	26.5–33.0		41.4	B94
	8.0	42.1	67	26.5–33.0		39.0	B94
	7.5	38.2	88	26.5–33.0		36.8	B94
	7.0	35.4	107	26.5–33.0		34.6	B94
EUVE J1925−565.....	9.5	58.0	33	48.2	Spectroscopy	...	
	9.0	51.4	53	48.7		45.4	B94
	8.5	46.0	77	49.5		40.8	B94
	8.0	41.8	105	51.0		37.0	B94
	7.5	38.8	142	...		33.8	B94
	7.0	35.8	173	...		31.3	B94
EUVE J2126+193.....	9.5	40.2	31	35.2	Spectroscopy	...	
	9.0	36.2	45	35.5		35.5, 35.6	L93, B94
	8.5	33.4	63	35.7		32.7, 32.7	L93, B94
	8.0	31.0	82	36.0		30.5, 30.8	L93, B94
EUVE J2300−070.....	9.5	49.5	42	30.0–50.0	Photometry	...	
	9.0	44.0	62	30.0–50.0	log g = 7.0–9.5	40.9	B94
	8.5	40.0	90	30.0–50.0		36.9	B94
	8.0	36.5	120	30.0–50.0		34.4	B94
	7.5	34.0	157	30.0–50.0		32.3	B94
	7.0	31.5	180	30.0–50.0		30.2	B94
EUVE J2353−703.....	9.0	72.3	51	...	Spectroscopy	80.2	B94
	8.5	64.0	75	...		68.0	B94
	8.0	57.6	105	~70.0		69.3	B94
	7.5	53.0	148	...		59.9	B94
	7.0	49.3	198	...		53.8	B94

REFERENCES.—B94 = Barstow et al. 1994; B97 = Burleigh et al. 1997; L93 = Landsman et al. 1993.

TABLE 8

RADIAL VELOCITIES

UT Date (1)	HJD (2,450,000+) (2)	v_{rad} (km s^{-1}) (3)	UT Date (4)	HJD (2,450,000+) (5)	v_{rad} (km s^{-1}) (6)
		HD 15638			
1997 Nov 19.....	772.07021	−1.1	1997 Dec 04	787.05435	−0.9
	772.14798	−1.2	1997 Dec 29	812.05199	+0.6
		HD 18131			
1995 Oct 19	9.87592	+15.0	1996 Sep 21	347.89566	+19.7
1995 Oct 20	10.76426	+15.3	1996 Oct 12	369.00369	+18.5
	10.94835	+13.9	1996 Oct 13	369.84830	+20.7
1995 Nov 28.....	49.74076	+17.6		369.91894	+20.1
	49.81905	+16.9	1996 Oct 22	378.84392	+18.3
1995 Nov 29.....	50.71650	+16.3	1996 Nov 12	399.80784	+19.5
1995 Nov 30.....	51.66392	+16.0		399.84433	+19.9
	51.78772	+16.1	1996 Nov 13	400.83777	+19.4
1995 Dec 24	75.77311	+16.2		400.88692	+19.3
1996 Aug 17.....	313.01896	+18.7	1997 Jan 12	460.62566	+18.4
1996 Aug 18.....	313.96413	+20.1	1997 Feb 9	488.62417	+18.8
1996 Sep 20	346.89265	+18.3			
		HR 1608			
1995 Oct 19	9.99269	−12.2	1996 Mar 20	162.63367	−11.9
1995 Oct 20	10.92685	−13.2	1996 Sep 20	347.01454	−20.8
1995 Nov 28.....	49.80314	−11.3	1996 Sep 21	347.97013	−19.9
	49.99345	−11.8	1996 Oct 12	369.03355	−20.6
1995 Nov 29.....	50.74672	−11.6	1996 Oct 13	369.93463	−19.7
	50.97072	−11.8	1996 Oct 22	378.88992	−22.3
1995 Nov 30.....	51.77434	−11.7	1996 Nov 12	399.98490	−20.7
	51.87970	−12.4	1997 Jan 12	460.72109	−19.0
1995 Dec 24	75.78963	−12.8	1997 Feb 9	488.65446	−18.9
	75.94201	−13.1	1997 Mar 10	517.62072	−16.9
1996 Jan 23.....	105.86012	−10.2	1997 Mar 12	519.63287	−17.3
1996 Mar 19.....	161.65085	−13.0	1997 Dec 2	784.88836	−10.4
		HD 33959C			
1995 Oct 19	9.97574	+16.1	1995 Nov 30	51.69958	+9.4
	10.01315	+17.8		51.80578	+13.8
	10.02621	+17.8		51.81825	+14.2
	10.03854	+18.7		51.90111	+17.2
1995 Oct 20	10.89193	−7.3		51.91324	+17.6
	10.90685	−7.3		52.02420	+19.7
	10.96947	−12.1		52.03652	+19.7
	10.98145	−12.1		52.07220	+19.1
	11.04596	−15.9		52.08573	+20.0
	11.06060	−17.7	1995 Dec 12	75.73278	+13.7
1995 Nov 28.....	49.75722	−2.0		75.81992	+17.2
	49.77001	−2.5	1996 Jan 23	105.82995	+18.7
	49.83700	−6.8		105.83900	+20.1
	49.84898	−8.2		105.87319	+21.9
	50.01107	−17.2		105.88226	+20.0
	50.02613	−17.7	1996 Mar 19	161.66679	−33.1
1995 Nov 29.....	50.76290	−38.2		161.67767	−31.7
	50.77484	−36.4	1996 Sep 20	346.93512	−38.0
	50.86990	−34.3		346.96817	−38.1
	50.88281	−33.9	1996 Sep 21	347.93679	+5.3
	50.98813	−30.0	1996 Oct 12	368.93065	+7.8
	51.00607	−29.1		368.96433	+10.0
1995 Nov 30.....	51.68723	+9.0	1997 Feb 9	488.67950	+10.5
		HD 33959A			
1995 Oct 19	10.00330	−28.3	1996 Jan 23	105.84606	−16.5
1995 Oct 20	10.96000	−24.8	1996 Mar 20	162.66072	−16.6
1995 Nov 28.....	49.77880	+11.7	1996 Sep 20	346.95071	−22.9
	50.03538	+13.4	1996 Sep 21	347.95236	−24.9
1995 Nov 29.....	50.78438	+3.4	1996 Oct 12	368.94508	+6.9
1995 Nov 30.....	51.92166	−31.7	1997 Feb 9	488.69763	−7.4
		EUVE J0702+129A			
1995 Nov 28.....	49.91892	−9.8	1996 Oct 22	379.02232	−11.5
	49.96216	−9.5		379.05553	−12.0

TABLE 8—*Continued*

UT Date (1)	HJD (2,450,000+) (2)	v_{rad} (km s^{-1}) (3)	UT Date (4)	HJD (2,450,000+) (5)	v_{rad} (km s^{-1}) (6)
		EUVE J0702+129A			
1995 Nov 29	50.93016	−9.6	1996 Nov 12	399.88317	−12.1
	51.04367	−9.7		399.92703	−11.0
1995 Nov 30	51.85134	−8.9	1996 Dec 17	434.91053	−12.0
	51.94704	−10.1		434.99555	−12.2
	51.99043	−9.3	1996 Dec 18	435.90904	−10.5
1995 Dec 24	75.85670	−10.0		435.99734	−9.8
1996 Oct 22.....	378.97907	−10.7			
		θ Hya			
1995 Nov 28	50.03868	−15.1	1996 Apr 19	192.69516	−22.4
1995 Nov 29	50.95445	−16.0		192.72425	−22.0
	51.06718	−15.4	1996 May 23	226.70602	−22.4
1995 Nov 30	51.88771	−15.1	1996 Jun 24	258.67793	−23.7
	52.04291	−16.8		258.68636	−27.3
1995 Dec 24	75.88684	−18.1	1996 Nov 12	400.04675	−19.5
1996 Jan 23	105.92515	−12.5	1996 Dec 17	435.04868	−21.0
1996 Mar 19	161.79712	−22.1	1996 Dec 19	436.84947	−13.4
	161.80872	−21.2	1997 Mar 12	519.76275	−17.2
1996 Mar 20	162.69636	−17.2			
		BD +27°1888			
1996 Mar 19	161.85614	+15.1	1997 Jan 8	457.08326	−0.7
1996 Mar 20	162.88734	+17.8	1997 Jan 9	457.99365	+3.7
1996 May 24.....	227.76454	+8.0	1997 Mar 12	519.79559	+0.7
1996 Dec 17	435.08591	−0.9			
		β Crt			
1995 Dec 24	75.89258	+7.0	1996 Mar 20	162.85465	+10.1
	75.95218	+6.0		162.92917	+9.5
1996 Jan 23	105.89715	+9.1	1996 Apr 19	192.74726	+9.0
	105.91076	+9.5		192.76035	+9.0
	105.99442	+9.3		192.87164	+8.7
	106.00892	+9.3	1996 May 24	227.67100	+9.9
1996 Mar 19	161.82240	+8.9		227.73493	+10.2
	161.83131	+8.4	1996 Dec 17	435.11257	+9.8
	161.87865	+9.2	1997 Feb 9	488.83629	+5.7
	161.88832	+8.7	1997 Mar 12	519.91601	+5.7
1996 Mar 20	162.78060	+10.8		519.92456	+5.2
	162.79385	+9.9			
		HR 8210			
1995 Oct 19.....	9.65942	−12.0	1996 Jul 12	276.84632	−53.2
	9.78005	−12.2	1996 Jul 21	285.77662	+35.3
1995 Oct 20.....	10.64933	−26.4		285.78878	+35.3
1995 Nov 28	49.61956	+29.3		285.86443	+34.7
	49.66174	+26.5	1996 Jul 22	286.77002	+35.4
1995 Nov 29	50.59087	+18.9		286.78198	+35.4
	50.59763	+19.3		286.91163	+34.6
1995 Nov 30	51.58720	+6.6	1996 Aug 17	312.69390	+0.6
	51.59647	+7.0		312.71033	+2.4
1996 May 23.....	226.92453	−12.4		312.94520	−0.5
1996 May 24.....	227.93911	−25.7	1996 Aug 18	313.73090	−11.8
1996 Jun 23.....	257.82375	−29.2		313.74633	−12.3
1996 Jun 24.....	258.86367	−15.8	1996 Sep 20	346.67631	−2.2
	258.88968	−14.5	1996 Sep 21	347.65727	+10.3
1996 Jul 7	271.82482	−31.0	1996 Oct 12	368.64706	+0.3
	271.99992	−32.8	1996 Oct 13	369.65646	+12.8
1996 Jul 8	272.83252	−41.8		369.73144	+14.4
1996 Jul 9	273.82737	−51.5	1996 Nov 12	399.64321	+2.3
1996 Jul 10.....	274.82681	−53.4		399.66233	+3.2
1996 Jul 11.....	275.81903	−55.1	1996 Nov 13	400.64468	−9.6
	275.83969	−56.0	1997 Jun 6	605.98420	−21.6
1996 Jul 12.....	276.79762	−53.1	1997 Jun 7	606.89470	−8.3
	276.81335	−54.0		606.90331	−9.2
		HD 217411			
1995 Oct 19.....	9.72623	+23.1	1996 Jul 12	276.92029	+22.2
	9.84179	+22.8	1996 Jul 22	286.89130	+21.7
1995 Oct 20.....	10.86559	+27.4	1996 Aug 17	312.77007	+22.7

TABLE 8—*Continued*

UT Date (1)	HJD (2,450,000+) (2)	v_{rad} (km s^{-1}) (3)	UT Date (4)	HJD (2,450,000+) (5)	v_{rad} (km s^{-1}) (6)
		HD 217411			
1995 Nov 28.....	49.69444	+23.3		312.82174	+22.6
1995 Nov 29.....	50.62933	+22.5	1996 Aug 18	313.82271	+22.6
1995 Nov 30.....	51.62706	+22.0		313.86850	+22.5
1996 Jun 23	257.90994	+23.0	1996 Sep 20	346.71075	+23.6
1996 Jul 8.....	272.99264	+21.8	1996 Sep 21	347.69172	+25.5
1996 Jul 9.....	273.99038	+23.4	1996 Oct 12	368.68747	+23.9
1996 Jul 10	275.00997	+23.5		368.75433	+21.9
1996 Jul 11	276.00899	+21.9	1996 Nov 13	400.68112	+23.1
		HD 223816			
1997 Nov 19.....	771.99500	+22.2	1997 Dec 04	787.00403	+21.1
	772.02209	+22.7	1997 Dec 27	809.93512	+23.4

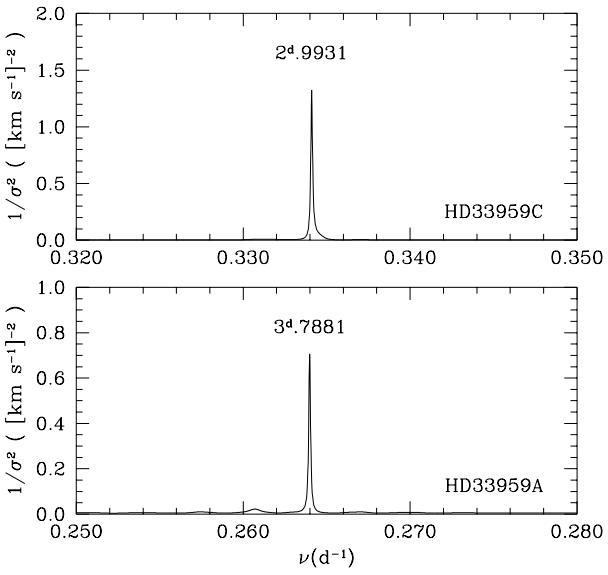

FIG. 6.—Search for periodicity in radial velocity measurements of the F2 V star in the binary HD 33959C (*top*) and the nearby A9 III + ? pair HD 33959A (*bottom*). The orbital period is marked.

mass function implies a white dwarf mass of only 0.29–0.42 $M_\odot$, assuming a F star mass between 1.2 and 1.5 $M_\odot$.

EUVE J0702+129A.—(Table 8; Fig. 9) Vennes et al. (1997a) recently reported the discovery of a white dwarf companion to a K0 IV–V star detected in the *ROSAT* WFC and *EUVE* surveys. Echelle spectroscopy of the K0 star shows no significant radial velocity variations with an average of -10.5 km s^{-1} and a standard deviation of 1.1 km s^{-1}.

θ Hya.—(Table 8; Fig. 8) We measured marginal radial velocity variations in the fast-rotating B star ($v_{rot} \sin i \sim 100$ km s^{-1}). The average radial velocity is -18.9 km s^{-1} with a standard deviation of 3.9 km s^{-1}.

BD +27°1888.—(Table 8; Fig. 8) We noticed possible variations in a small number of measurements ($\langle v_{rad} \rangle = +6.2$ km s^{-1} and $\sigma = 7.6$ km s^{-1}). The F star is a fast rotator, and the accuracy of the measurements is diminished.

β Crt.—(Table 8; Fig. 9) Campbell & Moore (1928) report velocity variations with a full amplitude of 20 km s^{-1} which prompted Fleming et al. (1991) to offer some speculations on possible orbital properties. Our measurements (23

TABLE 9

ORBITAL PARAMETERS

Name	P (days)	K (km s^{-1})	γ (km s^{-1})	f_{WD} ($M_\odot$)	M_{WD} ($M_\odot$)	e
HD 15638.....	...	<0.7	-0.7 ± 0.7	...	...	...
HD 18131.....	...	<1.9	$+18.0 \pm 1.9$	...	...	...
HR 1608	903 ± 5[a]	4.8 ± 0.5	-14.8 ± 0.4	0.009 ± 0.003	≥0.27[b]	0.30 ± 0.06[a]
HD 33959C.....	2.9931 ± 0.0001	29.4 ± 0.2	-9.3 ± 0.2	0.0079 ± 0.0002	≥0.25[c]	0
	2.99322 ± 0.00005[d]	...	...	...	...	...
HD 33959A.....	3.7881 ± 0.0003	24.0 ± 0.7	-8.7 ± 0.5	...	...	0
J0702+129A.....	...	<1.1	-10.5 ± 1.1	...	...	...
β Crt.....	...	<1.6	$+8.6 \pm 1.6$	...	...	...
HR 8210	21.722 ± 0.002	46.0 ± 0.3	-9.7 ± 0.2	0.219 ± 0.004	≥1.25[e]	0
	21.72168 ± 0.00009[f]	...	...	...	...	...
HD 217411	...	<1.3	$+23.0 \pm 1.3$	...	...	...
HD 223816	...	<0.8	$+22.4 \pm 0.8$	...	...	...

[a] From Beavers & Eitter 1988, quoted in Landsman et al. 1993.
[b] Assuming a minimum G5–K0 IV mass of 1.5 $M_\odot$.
[c] Assuming a minimum F2–6 IV/V mass of 1.2 $M_\odot$.
[d] Merging new data with Tokovinin's 1997 data.
[e] Assuming a minimum A6–8 V mass of 1.8 $M_\odot$.
[f] Merging new data with Harper's 1927 data.

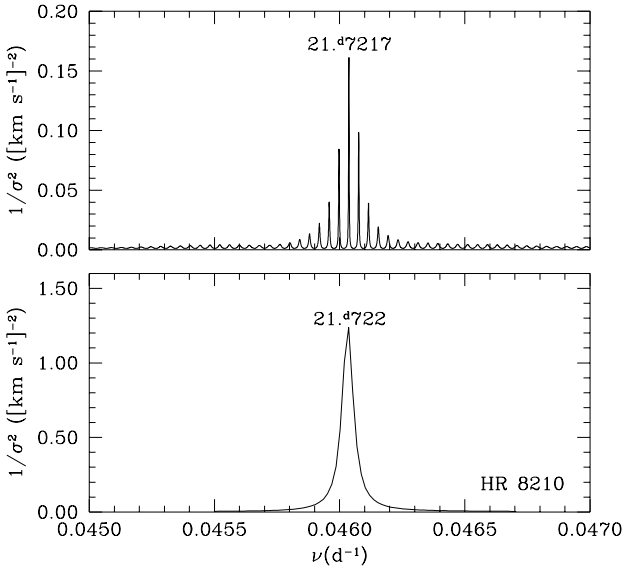

FIG. 7.—Search for periodicity in radial velocity measurements of the A8 V in the binary HR 8210 measured at Lick Observatory (*bottom*) and in combination with Dominion Astrophysical Observatory data (*top*; Harper 1927). The orbital period is marked.

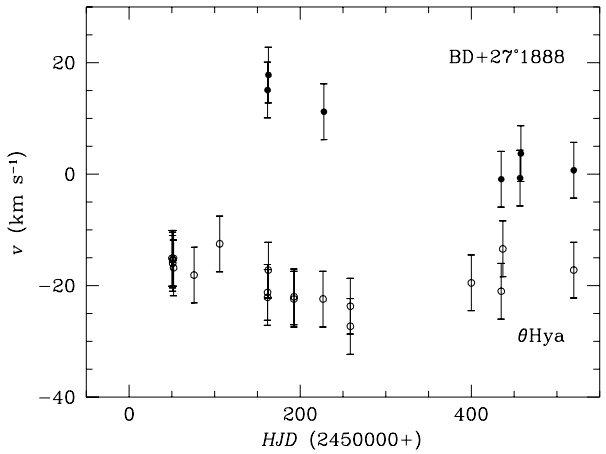

FIG. 8.—Radial velocity measurements of two rapidly rotating early–main-sequence stars, BD +27°1888 and θ Hya, showing possible long-term variations.

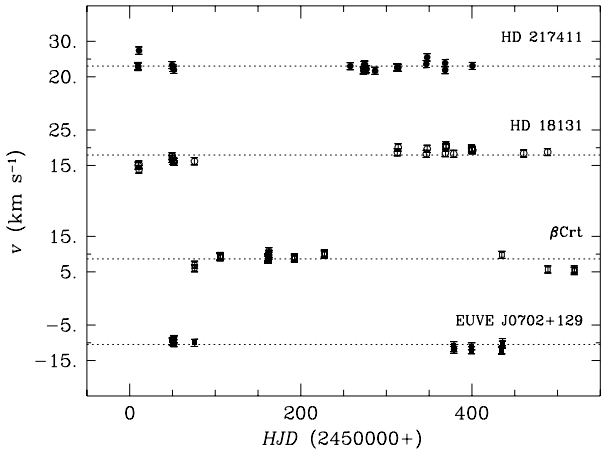

FIG. 9.—Radial velocity measurements of the secondary stars in the binaries HD 217411, HD 18131, β Crt, and EUVE J0702+129.

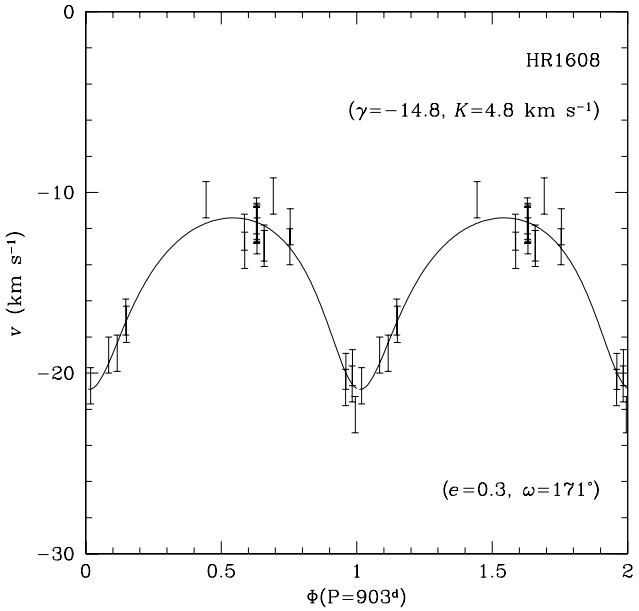

FIG. 10.—Radial velocity measurements of HR 1608 phased on Beavers & Eitter's (1988) orbital period and eccentricity. Phase zero corresponds to passage at periastron (T_0 = 24,450,384).

velocities) limit the orbital velocity amplitude to $K < 1.6$ km s^{-1}. The A1 III + DA binary β Crt is not a close binary, and monitoring over a period of 15 months only shows slight deviations from the systemic velocity $\gamma = +8.6 \pm 1.6$ km s^{-1}. Smalley et al. (1997) independently reached a similar conclusion based on a smaller sample of seven velocity measurements ($\gamma = +10.7 \pm 0.7$ km s^{-1}).

EUVE J1925−565A.—We have obtained a single measurement on 1997 November 20 (HJD 2,450,772.90641): $v_{\rm rad} = -14.3$ km s^{-1}. Additional measurements will be obtained in 1998–1999.

HR 8210.—(Table 8; Figs. 7 and 13) Landsman et al. (1993) and Wonnacott et al. (1993) identified the white

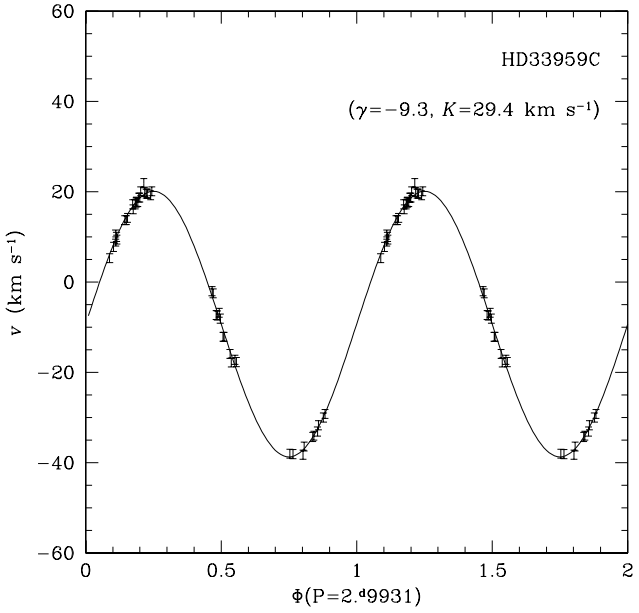

FIG. 11.—Radial velocity measurements of HD 33959C phased on the orbital period. Phase zero corresponds to passage at inferior conjunction (T_0 = 2,450,012.445).

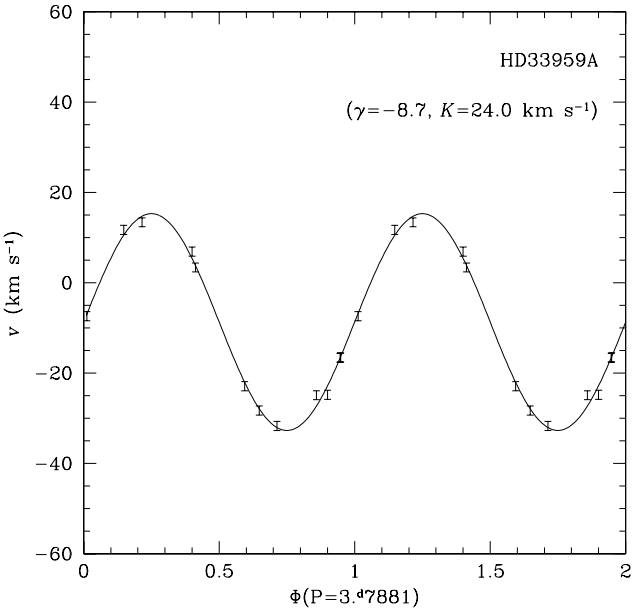

FIG. 12.—Radial velocity measurements of HD 33959A phased on the orbital period. Phase zero corresponds to passage at inferior conjunction (T_0 = 2,450,011.338).

dwarf primary, thereby resolving the long-standing mystery of the nature of the unseen companion. Our own velocity measurements (46 velocities) coupled with Harper's (1927) data (18 velocities) result in an accurate period of 21.72168 ± 0.00009 days, considerably refining the period based on contemporary data alone (see comparisons in Table 9). However, we only utilize recent measurements to determine the velocity amplitude and the mass function. Adopting a minimum mass of 1.8 $M_\odot$ for a A8 V secondary, we derive a minimum white dwarf mass of ~1.25 $M_\odot$. This limit depends, of course, on the mass adopted for the A star, but a comparison with the range of masses set by the *Hipparcos* parallax measurements shows that the inclination must be fairly high. Landsman, Simon, & Bergeron (1995) searched for but did not detect an eclipse of the white dwarf by the A star.

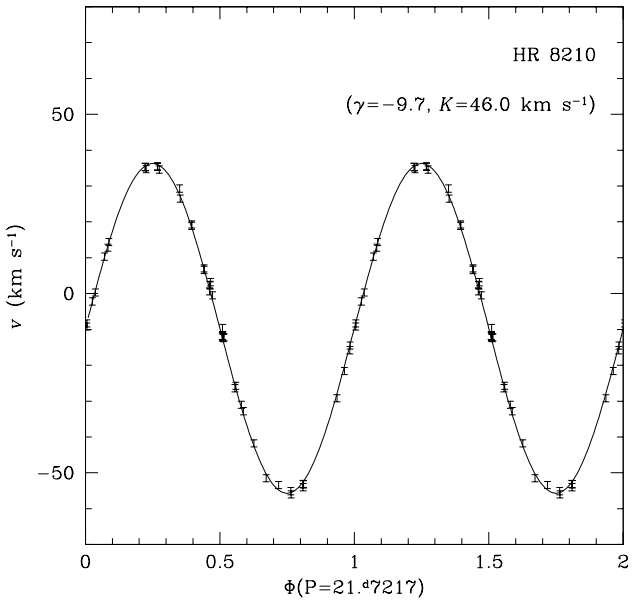

FIG. 13.—Radial velocity measurements of HR 8210 phased on the orbital period. Phase zero corresponds to passage at inferior conjunction (T_0 = 2,450,020.275).

HD 217411.—(Table 8; Fig. 9) We found no radial velocity variations in a long series of measurements: the average radial velocity is +23.0 km s^{-1} with a standard deviation of 1.3 km s^{-1}.

HD 223816.—(Table 8) A short series of four measurements obtained on three nights show a constant radial velocity with an average of +22.4 km s^{-1} and a standard deviation of 0.8 km s^{-1}.

Table 9 summarizes known orbital properties of the systems.

5. SUMMARY

We have presented multiwavelength observations of a sample of 13 binary systems selected from EUV surveys consisting of a DA white dwarf and a luminous secondary companion. We constrained the white dwarf temperatures and surface gravities using model atmosphere fits to *IUE* FUV spectra. The temperatures and neutral hydrogen column densities in the local ISM were further constrained by EUV photometric and spectroscopic measurements. We derived distances from white dwarf model atmosphere analyses, and these were, in a few cases, marginally consistent with distances derived from the absolute magnitude of the companion star. When available and demonstrably not affected by orbital motion, the *Hipparcos* parallax measurements help constrain the stellar properties. We find in particular that properties of the white dwarfs EUVE J0515+326 and EUVE J2126+193 are well constrained if one adopts (after assessing the effect of binary motion) the parallax measurements of HD 33959A and HR 8210, respectively. BD +27°1888 is a notable exception, and the white dwarf and F star may not constitute a physical pair. Radial velocity measurements allowed us to determine the orbital parameters of HD 33959C and HR 8210, and to measure long-period low-amplitude variations in five additional objects (HD 18131, HR 1608, θ Hya, BD +27°1888, and β Crt). The two binaries EUVE J0702+129 and HD 217411 showed no significant velocity variations above ~1 km s^{-1}; we have initiated radial velocity studies of HD 15638, EUVE J1925−565, and HD 223816. The study of all these objects will benefit from further EUV and FUV spectroscopy to determine better their effective temperature and surface gravity, and hence mass. Such determinations will help constrain the effect of binary evolution and, in particular, of a CE phase on the fate of stars involved in these processes.

In summary, we found that

1. Companions to white dwarf stars range from B main-sequence stars and A giants to K and M dwarfs. A positive identification of the white dwarf companion to the B9.5 V star θ Hya awaits EUV spectroscopy scheduled for 1998 with *EUVE*.

2. The FUV continuum and Lyα line profile measurements do not uniquely constrain $T_{\rm eff}$ and log g, but instead define a relation between the two parameters that can only be resolved if one adopts additional independent constraints. We partly resolved the ambiguity by adopting the distance toward the secondary star for the white dwarf, or by performing a model-atmosphere analysis of EUV continuum flux measurements (e.g., EUVE J1925−565). Table 10

TABLE 10

WHITE DWARF MASSES

Name	Binary	M_{WD} ($M_\odot$)
EUVE J0044+095.....	BD +08°102	0.9:
EUVE J0228−613.....	HD 15638	0.44–1.10
EUVE J0254−053.....	HD 18131	0.5:
EUVE J0459−102.....	HR 1608	0.51–0.67:
EUVE J0515+326.....	HD 33959C	0.30–0.69
		0.53–0.69[a]
EUVE J0702+129.....	...	0.32–0.93
EUVE J0914+023.....	θ Hya	?
EUVE J1024+263.....	BD +27°1888	0.34–0.93
EUVE J1111−228.....	β Crt	$\leq$0.44
EUVE J1925−565.....	...	0.70–0.76
EUVE J2126+193.....	HR 8210	1.00–1.32
		1.13–1.24[a]
EUVE J2300−070.....	HD 217411	0.68–1.16
EUVE J2353−703.....	HD 223816	0.60–0.95

[a] With distances set with *Hipparcos* parallax.

lists mass estimates, combining spectroscopic and orbital constraints, for the white dwarf stars (§ 3.2), showing that only one object (EUVE J2126+193) and possibly another one (EUVE J2300−070) out of 13 has a mass exceeding 1.1 $M_\odot$. Most objects fall within the range of masses estimated from the EUV-selected sample of isolated DA white dwarfs (Vennes et al. 1997b); the average mass, excluding EUVE J2126+193, is $M = 0.7\ M_\odot$, and the standard deviation is $\sigma_M = 0.2\ M_\odot$. Accurate luminosity class criteria would also help further constrain the distance toward the secondary star, but we find that *Hipparcos* parallax measurements generally corroborate our luminosity estimates.

3. A close DA + F (HD 33959C) and DA + A system (HR 8210) add to the sample of short-period DA + dM (e.g., Feige 24) and DA + dK (V471 Tau) binaries selected in EUV surveys. The period of HD 33959C is 2.99322 days and the period of HR 8210 is 21.72168 days, indicating that the two systems certainly emerge from a CE phase. The measured mass function limits the mass of the white dwarf in HD 33959C and HR 8210 to $\geq$0.25 and $\geq$1.25 $M_\odot$, respectively, assuming a mass of 1.2 and 1.8 $M_\odot$ for the secondary stars, respectively. The mass of the white dwarf in HD 33959C may be as low as 0.29–0.42 $M_\odot$, based on an estimate of the orbital inclination. Interestingly, the presence of two relatively early (and more massive) secondary stars in the sample has implications for the formation and evolution of binaries. De Kool & Ritter (1993) theorize that correlated initial mass functions for the binary members favor the formation of pairs with slightly more massive secondary stars, as opposed to binary members randomly associated. Although the selection criteria used in de Kool & Ritter's trials do not exactly apply to EUV-selected samples, we find evidence that close early-type companions to white dwarfs are almost as common as late-type companions.

4. The two systems HD 18131 and β Crt may have experienced radial velocity variations during our observation campaign. Such variations had already been noted in the system HR 1608 that limit the mass of the white dwarf to $\geq 0.27\ M_\odot$.

Additional observations are proposed:

1. The mass of the white dwarfs in these systems must be determined independently using the H Lyman line series in the FUV. This wavelength range will soon be explored in detail with the spectrometer aboard the *Far Ultraviolet Explorer* (*FUSE*). *ORFEUS* observations of the hot white dwarfs G191-B2B and MCT 0455−2812 (Vennes et al. 1996b) show the great potential of this wavelength range for the study of white dwarf properties.

2. Extreme-ultraviolet spectroscopy of the hot white dwarf is an effective means for temperature and chemical composition studies (e.g., EUVE J1925−565). Observations of β Crt and θ Hya with *EUVE*, which, in principle, will allow us to constrain their effective temperatures, are scheduled for 1998.

3. New and continued radial velocity studies of BD +08°102, HD 15638, HD 223816, and EUVE J1925−565 (Table 1) and MS 0354.6−3650 (Table 2) are planned for 1998–1999 using the echelle spectrometer at the MSO 74 inch telescope. These new observations will complete our sample as well as add interesting new cases (e.g., MS 0354.6−3650) to this investigation.

This work has been supported by NASA grant NAG5-2636 and NASA contract NAS5-30180. We express our gratitude to the Lick Observatory for generous allocation of time, and to the Lick Observatory staff (Mary and all) and Tony Misch for their careful and patient handling of the Berkeley fellows. We are also indebted to Mike Bessell at Mount Stromlo Observatory for sharing with us some of the secrets of the 74 inch telescope. This research has made use of the *Simbad* database.

REFERENCES

Abt, H. A., & Morrell, N. I. 1995, ApJS, 99, 135
Barstow, M. A., Holberg, J. B., Fleming, T. A., Marsh, M. C., Koester, D., & Wonnacott, D. 1994, MNRAS, 270, 499
Beavers, W. I., & Eitter, J. J. 1988, BAAS, 20, 737
Bernacca, P. L., & Perinotto, M. 1970, Contr. Oss. Astrof. Padova in Asiago, 239, 1
Bowyer, S., Lampton, M., Lewis, J., Wu, X., Jelinsky, P., & Malina, R. F. 1996, ApJS, 102, 129
Burleigh, M. R., Barstow, M. A., & Fleming, T. A. 1997, MNRAS, 287, 381
Campbell, W. W., & Moore, J. H. 1928, Publ. Lick Obs., 16, 167
Christian, D. J., Vennes, S., Thorstensen, J. R., & Mathioudakis, M. 1996, AJ, 112, 258
Dupuis, J., Vennes, S., Bowyer, S., Pradhan, A. K., & Thejll, P. 1995, ApJ, 455, 574
de Kool, M., & Ritter, H. 1993, A&A, 267, 397
ESA, 1997. The *Hipparcos* and Tycho Catalogues, ESA SP-1200
Favata, F., Barbera, M., Micela, G., & Sciortino, S. 1995, A&A, 295, 147
Fekel, F. C. 1997, PASP, 109, 514
Fleming, T. A., Schmitt, J. H. M. M., Barstow, M. A., & Mittaz, J. P. D. 1991, A&A, 246, L47
Génova, R., Bowyer, S., Vennes, S., Lieu, R., Henry, J. P., & Gioia, I. 1995, AJ, 110, 788
Gray, D. F. 1976, The Observation and Analysis of Stellar Photospheres (New York: Wiley), 398
Harper, W. E. 1927, Publ. Dom. Astrophys. Obs. Victoria, 4, 161
Heber, U., Bade, N., Jordan, S., & Voges, W. 1993, A&A, 267, L31
Hodgkin, S. T., Barstow, M. A., Fleming, T. A., Monier, R., & Pye, J. P. 1993, MNRAS, 263, 229
Houk, N., & Cowley, A. P. 1975, Michigan Spectral Survey, Vol. 1 (Ann Arbor: Univ. Michigan)
Jacoby, G. H., Hunter, D. A., & Christian, C. A. 1984, ApJS, 56, 257
Jeffries, R. D., Burleigh, M. R., & Robb, R. M. 1996, A&A, 305, L45
Jeffries, R. D., & Smalley, B. 1996, A&A, 315, L19
Jeffries, R. D., & Stevens, I. R. 1996, MNRAS, 279, 180
Kellett, B. J., et al. 1995, ApJ, 438, 364
King, A. R., Kolb, U., de Kool, M., & Ritter, H. 1994, MNRAS, 269, 907
Lampton, M., Lieu, R., Schmitt, J. H. M. M., Bowyer, S., Voges, W., Lewis, J., & Wu, X. 1997, ApJS, 108, 545
Landsman, W., Simon, T., & Bergeron, P. 1993, PASP, 105, 841
———. 1995, in White Dwarfs, ed. D. Koester & K. Werner (Berlin: Springer), 191

Montes, D., Fernández-Figueroa, M. J., De Castro, E., & Cornide, M. 1994, A&A, 285, 609
Mulliss, C. L., & Bopp, B. W. 1994, PASP, 106, 822
Nelson, B., & Young, A. 1970, PASP, 82, 699
Nichols, J. S., & Linsky, J. L. 1996, AJ, 111, 517
Pye, J. P., et al. 1995, MNRAS, 274, 1165
Roeser, S., & Bastian, U. 1988, A&AS, 74, 449
Schultz, G., Zuckerman, B., & Becklin, E. E. 1996, ApJ, 460, 402
Sion, E. M., Holberg, J. B., Barstow, M. A., & Kidder, K. M. 1995, PASP, 107, 232
Smalley, B., Kellett, B. J., Wonnacott, D., & Stickland, D. J. 1997, MNRAS, 284, 457
Smalley, B., Smith, K. C., Wonnacott, D., & Allen, C. S. 1996, MNRAS, 278, 688
Thejll, P., & Shipman, H. L. 1986, PASP, 98, 922
Thorstensen, J. R., Vennes, S., & Bowyer, S. 1996, ApJ, 457, 390
Thorstensen, J. R., Vennes, S., & Shambrook, A. 1994, AJ, 108, 1924
Tokovinin, A. A. 1997, A&AS, 121, 71
Tweedy, R. W., Holberg, J. B., Barstow, M. A., Bergeron, P., Grauer, A. D., Liebert, J., & Fleming, T. A. 1993, AJ, 105, 1398
Van Altena, W., & Sawada, K. 1983, AJ, 88, 1508
Vennes, S., Berghöfer, T., & Christian, D. J. 1997, ApJ, 491, L85
Vennes, S., Chayer, P., Hurwitz, M., & Bowyer, S. 1996b, ApJ, 468, 898
Vennes, S., Christian, D. J., Mathioudakis, M., & Doyle, J. G. 1997a, A&A, 318, L9
Vennes, S., Mathioudakis, M., Doyle, J. G., Thorstensen, J. R., & Byrne, P. B. 1995, A&A, 299, L29
Vennes, S., Thejll, P., Génova-Galvan, R., & Dupuis, J. 1997b, ApJ, 480, 714 (Paper II)
Vennes, S., Thejll, P., Wickramasinghe, D. T., & Bessell, M. S. 1996a, ApJ, 467, 782 (Paper I)
Vennes, S., & Thorstensen, J. R. 1994a, ApJ, 433, L29
———. 1994b, AJ, 108, 1881
———. 1995, in White Dwarfs, ed. D. Koester & K. Werner (Berlin: Springer), 313
———. 1996, AJ, 112, 284
Voges, W., et al. 1997, http://www.rosat.mpe-garching.mpg.de/survey/rass-bsc/
Vogt, S. S. 1987, PASP, 99, 1214
Webbink, R. F., Guinan, E. F., Koch, R. H., Kondo, Y., Etzel, P. B., & Thrash, T. A. 1992, BAAS, 24, 1127
Wonnacott, D., Kellett, B. J., & Stickland, D. J. 1993, MNRAS, 262, 277
Wood, M. A. 1995, in White Dwarfs, ed. D. Koester & K. Werner (Berlin: Springer), 41